An Investigation of the Dynamics of Several Equidistribution Schemes

Belinda Neil

September, 1994

Submitted to The University of Reading,

Department of Mathematics,

in part fulfillment of the requirements for the

Degree of Master of Science.

Abstract

In order to reduce computation costs in solving Partial Differential Equations (PDEs) whose solutions possess steep gradients or complex wave interactions, it can be important to use an adaptive computational grid which will move to resolve features of the solution. Many such adaption techniques are based on the principle of equidistribution, where some property of the PDE is distributed evenly on the grid. However it is known that some implementations of equidistribution can behave dynamically quite differently from the true solution. Here we study three such techniques, numerically and where possible analytically, both in the context of grid generation, where a grid is fitted to a given function, and as part of an adaptive strategy in solving a time-dependent PDE to steady state. In both cases a wealth of dynamical behaviour is uncovered.

Acknowledgements

I would like to thank Dr. P. K. Sweby for his help, support and advice during this work.

I would also like to acknowledge the financial support of the EPSRC.

Contents

Chapter 1

Introduction

In many applications of Computational Fluid Dynamics (CFD), it is necessary to solve Partial Differential Equations (PDEs) which do not possess analytic solutions. Some problems may have steep gradients, or complex shock wave interactions. For example, shock waves in compressible flow, combustion fronts, or classical boundary layers.

An important consideration when solving such PDEs is how to choose a non-uniform mesh which will suitably adapt to the solution behaviour. That is, one which follows and resolves local non-uniformities. A globally fine grid would be able to do this, but the high computing cost makes this impractical.

Several such techniques for obtaining non-uniform meshes are based on the equidistribution principle, i.e. where the mesh is moved so that a particular quantity is equally distributed over the domain. However, it is known that some of these mesh equidistribution schemes for time-dependent partial differential equations can experience instability (see, for example, [3], [2] and [5]).

In this dissertation we investigate numerically, and where possible analytically,

the dynamics of three implementations of equidistribution. First, we examine the effect of the equidistribution implementation alone by fitting a grid to known functions. Then we use equidistribution as part of an adaptive technique to solve time-dependent PDEs to steady state. We investigate two PDEs, one whose solution involves a steep gradient, and one with a boundary layer.

First we formalise what we mean by equidistribution, before we look in detail in Chapter 2 at three implementations, and investigate their dynamics in Chapter 4, both numerically and analytically. In Chapter 5 we apply two of the techniques to steady state solutions of two PDEs, and finally in Chapter 6 we summarise and discuss all of the results.

1.1 What is equidistribution?

The idea of equidistribution is to "distribute equally" a positive definite weight function, $w(x)$ on a grid (or mesh). If $w(x)$ is some measure of the error, common sense says that it would be a good idea to choose a mesh $\pi : a = x_0 < x_1 < \cdots < x_{N-1} < x_N = b$ such that the contributions to the error from each mesh subinterval (x_k, x_{k+1}) is the same. This is the basic idea of equidistribution.

If we are adapting a grid to the evolving solution of a PDE, as opposed to a known function, the weight function will be in terms of time also. So, mathematically, in one space dimension, we wish to find a moving mesh $\pi : a = x_0 < x_1(t) < \cdots < x_{N-1}(t) < x_N = b$, where $a = x_0$ and $b = x_N$ are the fixed boundary points, which equidistributes $w(x,t)$ for all values of t, i.e. we require

$$\int_{x_{k-1}}^{x_k} w(x,t)dx = \int_{x_k}^{x_{k+1}} w(x,t)dx = \frac{1}{N}\int_{x_0=a}^{x_N=b} w(x,t)dx \qquad (1.1)$$

for $k = 1, 2, \ldots, N$, and each value of t.

(There are other equivalent forms of expressing equidistribution, see for example Equations (2.6) and (2.30)).

1.2 The Weight Function

The weight, or monitor, function w will reflect some property of the underlying function u, to which the mesh is being fitted. For straightforward equidistribution both w and u will be functions of x, whilst for grid adaption in PDE solutions both will be functions of x and t. Examples of monitor functions are

(i) an arclength weight function,

$$w(x,t) = \sqrt{1 + u_x^2(x,t)} \tag{1.2}$$

(ii) a curvature weight function,

(iii) a combination of gradient and curvature,

(iv) truncation error or solution residual of the PDE.

Chapter 2

Implementations

In this section we consider various ways in which the equidistribution process can be implemented.

Grid adaption techniques based on equidistribution are usually applied to time-dependent PDE's by either

(i) Solving Equation (1.1) sequentially with the solution of the PDE, i.e. one PDE solver time-step followed by a regridding step(s), or

(ii) developing a system of Ordinary Differential Equations (ODEs) for the mesh velocities that are equivalent to Equation (1.1) and then solving the resulting coupled system of equations for both mesh location and PDE solution simultaneously.

The techniques we consider are all iterative techniques. The first directly approximates Equation (1.1), whilst the second and third involve deriving PDEs from (1.1).

2.1 Tridiagonal Iteration

In each interval (x_{k-1}, x_k), we approximate the weight function $w(x,t)$ to be constant. Equation (1.1) then becomes

$$w(x,t)_{k-\frac{1}{2}}(x_k - x_{k-1}) = w(x,t)_{k+\frac{1}{2}}(x_{k+1} - x_k), \qquad k = 1, \ldots, N-1. \tag{2.1}$$

and substituting in our monitor function (1.2), we get

$$\left(\sqrt{1+u_x^2}\right)_{k-\frac{1}{2}}(x_k - x_{k-1}) = \left(\sqrt{1+u_x^2}\right)_{k+\frac{1}{2}}(x_{k+1} - x_k), \qquad k = 1, \ldots, N-1. \tag{2.2}$$

From the way in which this is defined it is impossible for the nodes x_k to cross. Since $w(x,t)$ is always positive, then, if $x_{k+1} - x_k$ and $x_k - x_{k-1}$ are positive for the initial grid, they must always remain positive.

When using known functions, or when the analytic steady-state solution of the PDE is known, the exact derivative can be used. However, when the derivative is not known, we can approximate u_x by

$$u_x|_{k-\frac{1}{2}} \approx \frac{u_k - u_{k-1}}{x_k - x_{k-1}}. \tag{2.3}$$

Rearranging Equation (2.2) we get

$$\sqrt{1+u_x|^2_{k+\frac{1}{2}}}\,x_{k+1} - \left(\sqrt{1+u_x|^2_{k+\frac{1}{2}}} + \sqrt{1+u_x|^2_{k-\frac{1}{2}}}\right)x_k + \sqrt{1+u_x|^2_{k-\frac{1}{2}}}\,x_{k-1} = 0 \tag{2.4}$$

$k = 1, \ldots, N-1$.

The $\{x_k\}$ used to calculate the derivative, either exactly or approximately, are the nodal positions in the *existing* grid. Equation (2.4) is therefore linear in $\{x_k\}$ which represent a new grid, thereby forming an iteration

$$w^n_{k+\frac{1}{2}}x^{n+1}_{k+1} - (w^n_{k+\frac{1}{2}} + w^n_{k-\frac{1}{2}})x^{n+1}_k + w^n_{k-\frac{1}{2}}x^{n+1}_{k-1} = 0 \tag{2.5}$$

where superscripts denote iterates, and fixed end points are $x_0 = 0$ and $x_N = 1$. At each stage of the iteration a tridiagonal system must be solved.

2.2 Ren and Russell Iteration

This is an iterative method for solving a new equidistribution PDE derived from Equation (1.1). This scheme was derived in [3] as a method for solving a PDE, so when considering it as an iterative method for equidistributing a known function, we use the idea of artificial time.

Equation (1.1) can be rewritten in an equivalent form as

$$\int_{x_0}^{x_k(t)} w(x,t)dx = \frac{k}{N}\int_{x_0}^{x_N} w(x,t)dx \equiv \frac{k}{N}\theta(t), \tag{2.6}$$

where $\theta(t)$ is a function which Ren and Russell describe as representing the rate at which the mesh moves with time.

Replacing (x,t) in the original PDE by a new set of computational coordinates (s,T), defined by

$$s = \frac{1}{\theta}\int_{x_0}^{x} w(\xi,t)d\xi,$$

$$T = t. \tag{2.7}$$

yields a new system to be solved to find the equidistributing mesh. Ren and Russell use this transformation to derive a PDE which provides a new formulation of equidistribution. Rearranging the first equation of (2.7) gives

$$s\theta(t) = \int_{x_0}^{x} w(\xi,t)d\xi, \tag{2.8}$$

and assuming $w(\xi,t)$ is a smooth function, they differentiate along lines where

$s(t)$ is constant with respect to time, to obtain

$$s_t\theta + s\dot{\theta} = \int_{x_0}^{x} w_t(\xi, t)d\xi + w\dot{x}, \tag{2.9}$$

i.e.

$$s\dot{\theta} = \int_{x_0}^{x} w_t(\xi, t)d\xi + w\dot{x}. \tag{2.10}$$

Differentiating this with respect to x, gives

$$s_x\dot{\theta} + s\theta_x = w_t(x, t) + \frac{\partial}{\partial x}(w\dot{x}) \tag{2.11}$$

which, since θ is a function of t only, becomes

$$s_x\dot{\theta} = w_t(x, t) + \frac{\partial}{\partial x}(w\dot{x}). \tag{2.12}$$

Finally differentiating Equation (2.8) with respect to x and substituting in Equation (2.12), Ren and Russell obtain

$$\frac{\partial}{\partial t}w(x, t) + \frac{\partial}{\partial x}(w(x, t)\dot{x}) = \frac{\dot{\theta}(t)}{\theta(t)}w(x, t). \tag{2.13}$$

This is the new equidistribution PDE which is studied by Ren and Russell. They look at two different implementations of Equation (2.13) and investigate the stability. In the second of these implementations, the one we shall be considering, they introduce the transformation

$$W(x, t) = \frac{w(x, t)}{\theta(t)} = \frac{w(x, t)}{\int_{x_0}^{x_N} w(x, t)dx}, \tag{2.14}$$

where $W(x, t)$ is an "average energy" function.

Equation (2.13) then becomes

$$\frac{\partial}{\partial t}(W(x, t)\theta(t)) + \frac{\partial}{\partial x}(W(x, t)\theta(t)\dot{x}) = \frac{\dot{\theta}(t)}{\theta(t)}W(x, t)\theta(t), \tag{2.15}$$

i.e.

$$\frac{\partial W(x,t)}{\partial t}\theta(t) + W(x,t)\dot{\theta}(t) + \frac{\partial}{\partial x}(W(x,t)\dot{x}(t))\theta(t) + W(x,t)\dot{x}\theta_x(t) = \dot{\theta}(t)W(x,t). \tag{2.16}$$

Therefore, since θ is a function only of t, this yields

$$\frac{\partial W(x,t)}{\partial t} + \frac{\partial}{\partial x}(W(x,t)\dot{x}) = 0, \tag{2.17}$$

and to discretise this equation, Ren and Russell approximate the spatial derivatives over $[x_k, x_{k+1}]$ at $t = t^{n+1} = (n+1)\Delta t$ by

$$\frac{W_k^{n+1} - W_k^n}{dt} + \frac{W_k^{n+1}\dot{x}_{k+1} - W_{k-1}^{n+1}\dot{x}_k}{x_{k+1} - x_k} = 0. \tag{2.18}$$

Rearranging gives

$$W_k^{n+1}(x_{k+1} - x_k) + \Delta t(W_k^{n+1}\dot{x}_{k+1} - W_{k-1}^{n+1}\dot{x}_k) = (x_{k+1} - x_k)W_k^n, \tag{2.19}$$

and a similar approximation on $[x_{k-1}, x_k]$ yields

$$W_{k-1}^{n+1}(x_k - x_{k-1}) + \Delta t(W_{k-1}^{n+1}\dot{x}_k - W_{k-2}^{n+1}\dot{x}_{k-1}) = (x_k - x_{k-1})W_{k-1}^n. \tag{2.20}$$

Equidistribution implies, (see Equation (2.17)),

$$\int_{x_k}^{x_{k+1}} W(x,t)dx = \int_{x_{k-1}}^{x_k} W(x,t)dx, \tag{2.21}$$

and so, equating the right-hand side of Equation (2.19) and Equation (2.20), which are approximations to Equation (2.21) at $t = t^n$, they obtain

$$\begin{aligned} W_k^{n+1}(x_{k+1} - x_k) + \ & \Delta t(W_k^{n+1}\dot{x}_{k+1} - W_{k-1}^{n+1}\dot{x}_k) = \\ & W_{k-1}^{n+1}(x_k - x_{k-1}) + \Delta t(W_{k-1}^{n+1}\dot{x}_k - W_{k-2}^{n+1}\dot{x}_{k-1}). \end{aligned} \tag{2.22}$$

Since each term involves $W(x, t^{n+1}) = \frac{w(x,t^{n+1})}{\theta(t^{n+1})}$, $\theta(t^{n+1})$ can be eliminated, leaving the discrete approximation

$$\Delta t(w_k\dot{x}_{k+1} - 2w_{k-1}\dot{x}_k + w_{k-2}\dot{x}_{k-1}) = w_{k-1}(x_k - x_{k-1}) - w_k(x_{k+1} - x_k) \tag{2.23}$$

at $t = t^{n+1}$.

We use the same weight function as before, i.e.

$$w(x,t) = \sqrt{1 + u_x^2(x,t)}. \tag{2.24}$$

As stated earlier, this will be known exactly when the analytic steady-state solution $u(x,t)$ of the PDE is known, hence,

$$w_k = \sqrt{1 + u_x^2(x,t)|_k}. \tag{2.25}$$

But, when this is not known, we use the same discretisation as suggested in [3], namely

$$w_k = \sqrt{1 + \left(\frac{u_{k+1} - u_k}{x_{k+1} - x_k}\right)^2} \qquad k = 0, \ldots, N-1. \tag{2.26}$$

We only consider the fixed boundary case where $\dot{x}_0 = \dot{x}_N = 0$, and $x_0 = 0$, $x_N = 1$.

To solve Equation(2.23) we assume that all of the x_k are the nodal positions in the existing grid. Hence, the right-hand side of Equation (2.23) can be calculated. We then solve the tridiagonal system for $\dot{x}_k$, and find the updated grid using Euler time-stepping

$$x_k^{n+1} = x_k^n + \Delta t \dot{x}_k, \qquad k = 0, \ldots, N-1. \tag{2.27}$$

For the case of equidistributing a grid to a given function, as opposed to the adaptive solution of a PDE we can view time in (2.23) as an iteration or relaxation parameter. This is one of the iterative methods which we will use in this dissertation to perform equidistribution. We will refer to this as the Ren and Russell iteration.

Note that monotonicity is not ensured using this method, so it is possible for the nodes to cross.

2.3 Nominal Iteration

This iterative method is derived in [4]. The authors look at the problem from a variational point of view, but also show that this is equivalent to an equidistribution formulation.

In [4] it is noted that the equation for defining a grid with respect to a position dependent weight $w(x,t)$ is given by

$$x'(\xi)w(x(\xi),t) = \text{Constant}. \tag{2.28}$$

This can be seen by considering Equation (2.6) and reparameterising with $x = x(\xi)$ where $\xi \in [0,N]$ and $x_k = x(k)$. Hence

$$\int_{x_0}^{x(\xi)} w(x(\xi),t)d\xi = \frac{\xi}{N}\int_{x_0}^{x_N} w(x(\xi),t)d\xi, \tag{2.29}$$

which when differentiated with respect to ξ becomes

$$x'(\xi)w(x(\xi),t) = \frac{1}{N}\int_{x_0}^{x_N} w(x(\xi),t)d\xi = \text{Constant}, \tag{2.30}$$

as above.

Differentiating the above equation with respect to ξ gives a second order differential equation for $x(\xi)$ which is the same as the equation for the variational problem defining the adaptive grid,

$$x''(\xi) + \frac{\frac{\partial w}{\partial x}(x(\xi),t)}{w(x(\xi),t)}(x'(\xi))^2 = 0, \qquad x(0) = x_0, \quad x(N) = x_N. \tag{2.31}$$

This is the equation which is to be solved in order to equidistribute the grid. The iteration used is called in [4] the nominal iteration. It is

$$(x'')^{n+1} + (\frac{\frac{\partial w}{\partial x}(x(\xi),t)^n}{w(x,t)^n}(x')^n)(x')^{n+1} = 0, \qquad n \geq 0 \tag{2.32}$$

where n is the time level.

As before,

$$w(x,t) = \sqrt{1 + u_x^2(x,t)} \tag{2.33}$$

and so

$$\frac{\partial w}{\partial x}(x,t) = u_x(x,t)u_{xx}(x,t)(1 + u_x^2(x,t))^{-\frac{1}{2}}. \tag{2.34}$$

Hence, Equation (2.32) can be written as

$$x''_{j+1} + (\frac{u_x|_j u_{xx}|_j}{(1+u_x^2)_j} x'_j)x'_{j+1} = 0, \qquad j \geq 0, \tag{2.35}$$

where j denotes the iterate. If the analytic steady state of the PDE is known, or if a known function is being equidistributed, the first and second derivatives will be known exactly. This is the only case considered here, although it is possible to approximate the derivatives using finite differences when they are unknown.

In [4] Equation (2.35) the ξ derivatives are discretised using central differences and the equation solved using the existing nodal positions, to find the new nodal positions. Setting

$$\begin{aligned} g(x_j) &= \tfrac{u_x|_j u_{xx}|_j}{(1+u_x^2)_j} x'_j \\ &= \tfrac{u_x|_{k,j} u_{xx}|_{k,j}}{(1+u_x^2)_{k,j}} \left(\tfrac{x_{k+1,j} - x_{k-1,j}}{2\psi}\right), \qquad k = 1, \ldots, N-1, \quad j \geq 0 \end{aligned} \tag{2.36}$$

where $\psi = \frac{x_N - x_0}{N}$, we have

$$\frac{x_{k-1,j+1} - 2x_{k,j+1} + x_{k+1,j+1}}{\psi^2} + g(x_j)(\frac{x_{k+1,j+1} - x_{k-1,j+1}}{2\psi}) = 0, \tag{2.37}$$

$k = 1, \ldots, N-1$, the nodal positions, $j \geq 0$, the iterates, and $x_0 = 0, x_N = 1$. This can be written as a tridiagonal system, and then solved in the usual way to obtain the grid nodes at the next time level.

As with the Ren and Russell iteration, monotonicity is not ensured using this iterations, so it is possible for nodes to cross.

2.4 Exact Equidistribution

For comparison purposes, we want to know the "exact" placement of the grid nodes for the analytic steady state solution of the PDE. This can only be done exactly if the integral in (1.1) can be solved analytically. However, we find the "exact" placements sufficiently accurately by solving the integral using the trapezium rule, with a large number of subdivisions, i.e.

$$\frac{1}{N}\int_{x0}^{x_N} w(x,t)dx \approx \sum_{j=1}^{2000} \frac{1}{2}\Delta x(w_j + w_{j+1}) \qquad \Delta x \ll x_k - x_{k-1} \tag{2.38}$$

where j denotes the quadrature subintervals and $k = 1, \ldots, N-1$, numbers the free nodes.

Chapter 3

Methodology

We compare the dynamics of the three iterative techniques described in the previous chapter when used to equidistribute several test functions. Initially, we examine the dynamics of grid adaption alone by solving the regridding equations (2.4), (2.23), and (2.37) iteratively, using known functions (see Chapter 4).

We then solve the regridding equations and an underlying PDE simultaneously, and again examine the dynamics (see Chapter 5).

For the grid adaption alone, with certain functions, it was possible to investigate analytically the case of one free node, and also for the tridiagonal iteration, the case of two free nodes (see Sections 4.3, 4.4, 4.6). Mathematica was used as an aid in this analysis.

When looking at the grid adaption alone, all of the equidistribution methods were used with an odd number, 11, and an even number, 12, of free nodes. The tridiagonal iteration and the Ren and Russell iteration were applied using both the exact and the approximate derivative u_x. The nominal iteration was only solved using the exact derivative, due to a shortage of time.

For all of the test cases used, the "exact" placements of the grid nodes for the analytical steady state were found for comparison. This was done using quadrature, as described in Section 2.4.

All of the figures showing the results of applying the mesh equidistribution schemes are of α, or $\log_{10}(\alpha)$, against the equidistribed x. For each value of the parameter, α, we iterate 200 times and then plot the final 10 nodal positions for each node, overlaid on the same picture. If only one point can be seen at each node, the solution must have converged. If two points can be seen at any node there is a period 2 solution.

Due to the similarity of many of the results, only a few pictures are presented here, which illustrate the main features of the results. All of these pictures were created using Matlab, and all of the programs to perform the mesh equidistribution were written in Matlab.

Chapter 4

Equidistribution

4.1 Test Problems and Exact Results

Four different functions are used as test cases for the equidistribution techniques alone, where $f(x)$ takes the place of $u(x,t)$ in the equations in Chapter 2. They are :-

1. $f(x) = \alpha x(1-x)$: a quadratic function, see Figure 4.1 on the following page. This is a simple symmetric function.

2. $f(x) = \alpha x(\frac{1}{2} - x)(1-x)$: a cubic function, see Figure 4.2 on the following page. This is a simple unsymmetric function, but whose derivative is symmetric.

3. $f(x) = \frac{1-e^{x/\alpha}}{1-e^{1/\alpha}}$: an exponential function, see Figure 4.3. This is the steady state solution of the linear PDE solved Chapter 5 and represents a boundary layer.

4. $f(x) = A\tanh(\frac{A}{2\alpha}(x - \frac{1}{2})$ where $A\tanh(\frac{A}{4\alpha}) = 1$: a tanh function, see Figure 4.4. This is the steady state solution of the non-linear PDE solved in Chapter 5 and represents a steep front.

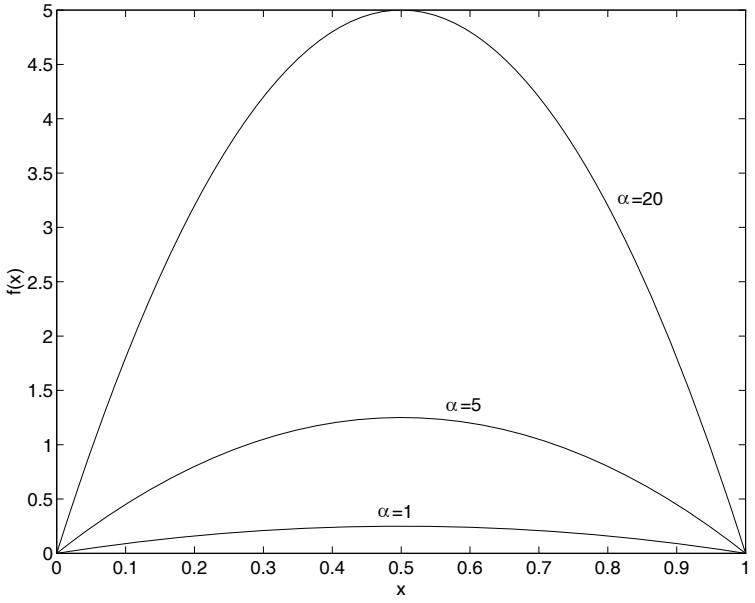

Figure 4.1: Quadratic Function.

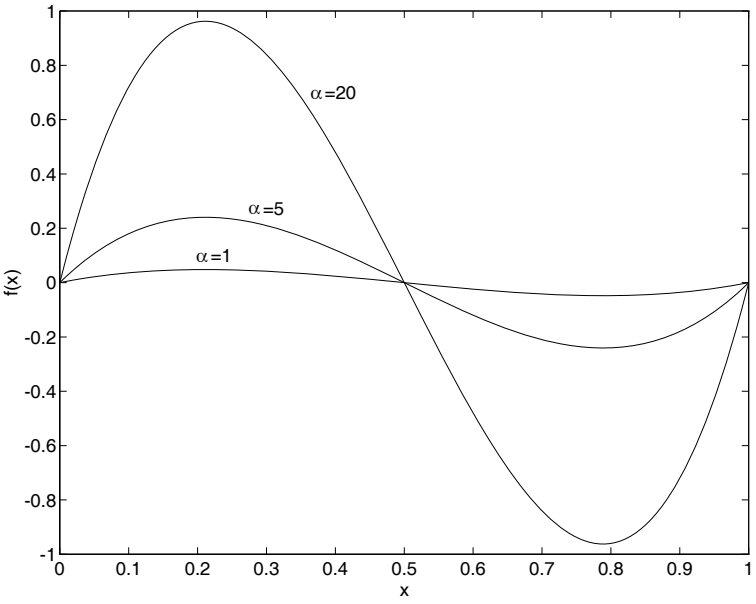

Figure 4.2: Cubic Function.

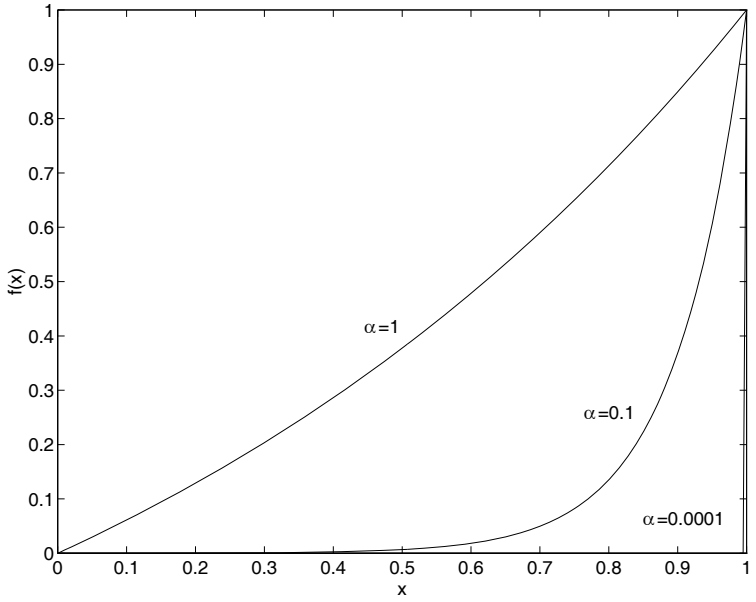

Figure 4.3: Exponential Function.

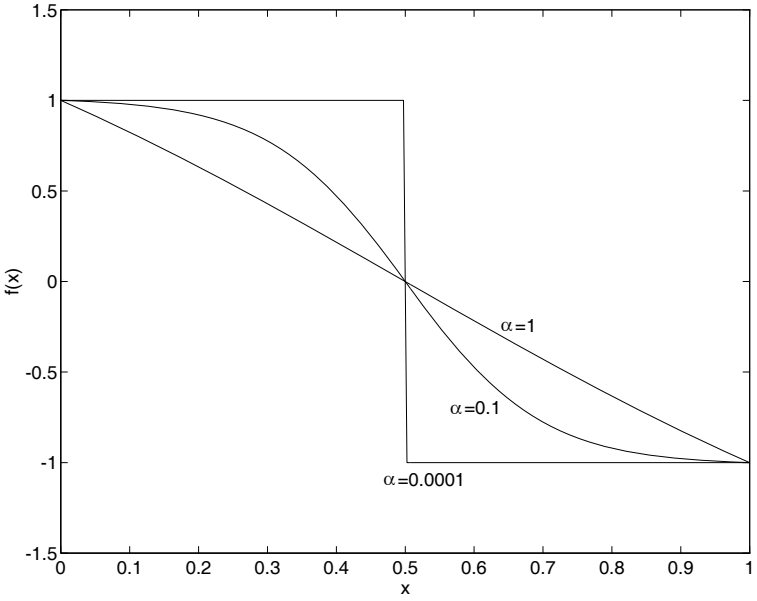

Figure 4.4: Tanh Function.

In each of these, α is a parameter that can be varied in order to investigate the dynamics of the equidistribution schemes. In the exponential function, as α decreases, the boundary layer becomes narrower. In the tanh function, as α decreases, the front becomes steeper.

For functions 1 and 2, the grid adaption schemes are applied for α in the range $[0.1, 20]$. In a few cases the range was extended to $\alpha \in [0.1, 50]$.

For functions 3 and 4, the schemes were applied for the range $\alpha \in [0.0001.1]$.

All of the equidistribution methods are used with a skewed initial grid ($x_0 = 0$, $x_1 = 0.01$, $x_2 = 2/N$, . . . ,$x_N = 1$ where $N+1$ is the number of grid points). The quadratic function is symmetric, and the cubic and tanh functions are symmetric in terms of equidistribution of arclength, i.e. when their derivative is squared, and thus for all three functions, symmetrical equidistribution of grid points is expected. However by starting with a skewed grid, it is more likely that non-symmetric solutions will be found, if they exist. The exponential function is non-symmetric, and so symmetric solutions are not expected.

4.2 Analysis

We begin the analysis by looking for fixed points $\overline{x}$ (also known as equilibrium points, critical points, or steady state solutions), of the iterative methods. The iterative process can be considered as a system of equations, one for each free node. However, since our analysis is confined to the case of a single free node, or a special case of two free nodes, scalar analysis suffices. Each of the methods can be written in the general form, $x^{n+1} = f(x^n)$. Fixed points are then the values $\overline{x}$ such that $x^n = \overline{x}$ for all n, and hence, $\overline{x} = f(\overline{x})$.

We now look at the method of perturbation to investigate the stability of the fixed points. By adding a small perturbation to the fixed point, we can find out whether the size of the perturbation will increase, i.e. the fixed point is unstable, or will decrease, i.e. the fixed point is stable.

Consider a small perturbation ϵ, $||\epsilon|| \ll 1$, from the fixed point $\overline{x}$, i.e.

$$x^n = \overline{x} + \epsilon. \tag{4.1}$$

Substituting this in Equation (4.2), and expanding using Taylor Series, we get

$$\begin{aligned} x^{n+1} = \overline{x} + \epsilon &= f(\overline{x} + \epsilon) \\ &= f(\overline{x}) + \epsilon f'(\overline{x}) + \tfrac{\epsilon^2}{2} f''(\overline{x}) + \dots \quad , \end{aligned} \tag{4.2}$$

and so

$$\epsilon = \epsilon f'(\overline{x}) + O(\epsilon^2). \tag{4.3}$$

To ensure that the magnitude of the perturbation decreases, we must bound $f'(\overline{x})$ such that

$$|f'(\overline{x})| < 1 \tag{4.4}$$

When this inequality is satisfied the fixed point will be stable.

If the inequality is greater than 1, the fixed point will be unstable, and for the case $|f'(\overline{x})| = 1$, linearised analysis does not give enough information to be able to determine stability.

By knowing the way in which a fixed point becomes unstable it is possible to tell something about its subsequent behaviour. One example, seen in Section 4.3.3, is when the fixed point becomes unstable with $f'(\overline{x}) = -1$. This indicates that the presence of a period doubling bifurcation, i.e. where $\epsilon^{n+1} \approx -\epsilon^n$, a period 2 solution. Alternatively, and this is seen in Sections 4.3.3 and 4.5, if $f'(\overline{x}) = 1$, a transcritical or pitch fork bifurcation will occur. To determine which particular type it is necessary to carry out an analysis of higher order terms (see for example [1]).

It is only possible to apply the analysis described to simple cases using the quadratic and cubic functions, even when using Mathematica as an aid.

4.3 Tridiagonal Iteration - Analysis

We consider the cases of one free node and two free nodes. We also consider the case where the derivative of the function is approximated, as well as the case where the exact derivative is used.

4.3.1 Quadratic Function : $f(x) = \alpha x(1-x)$

For this function we note first that the weight function using the exact derivative and the weight function using the approximate derivative are identical.

One free node

The one free node grid is given by $x_0 = 0$, $x_1 = X$, $x_2 = 1$. Hence $x_{\frac{1}{2}} = \frac{X}{2}$ and $x_{\frac{3}{2}} = \frac{1+X}{2}$. Consequently, using the exact derivative

$$f'(x) = \alpha(1-2x) \tag{4.5}$$

the weight functions are, from Equation (1.2),

$$\begin{aligned} w_{\frac{1}{2}} &= \sqrt{1+\alpha^2(1-X)^2}, \qquad \text{and} \\ w_{\frac{3}{2}} &= \sqrt{1+\alpha^2X^2}. \end{aligned} \tag{4.6}$$

If the approximate derivative given in Equation (2.3) is used, then

$$\begin{aligned} w_{\frac{1}{2}} &= \sqrt{1+(\tfrac{f(x_1)-f(x_0)}{x_1-x_0})^2} = \sqrt{1+\alpha^2(1-X)^2}, \qquad \text{and} \\ w_{\frac{3}{2}} &= \sqrt{1+(\tfrac{f(x_2)-f(x_1)}{x_2-x_1})^2} = \sqrt{1+\alpha^2X^2}. \end{aligned} \tag{4.7}$$

Clearly, the weight functions are the same using the exact and using the approximate derivatives.

We substitute in Equation (2.4), and find any fixed points of X by putting

$X^n = X^{n+1} = \overline{x}$. Hence,

$$\sqrt{1+\alpha^2\overline{x}^2}(1-\overline{x}) = \sqrt{1+\alpha^2(1-\overline{x})^2}\overline{x}, \tag{4.8}$$

then squaring both sides,

$$(1+\alpha^2\overline{x}^2)(1-2\overline{x}+\overline{x}^2) = (1+\alpha^2(1-\overline{x})^2)\overline{x}^2, \tag{4.9}$$

and eliminating terms leaves

$$1-2\overline{x} = 0 \tag{4.10}$$

i.e.

$$\overline{x} = \frac{1}{2}. \tag{4.11}$$

This is the only fixed point and we now analyse its stability. We find that

$$f'(\frac{1}{2}) = \frac{\alpha^2}{4\left(1+\frac{\alpha^2}{4}\right)}, \tag{4.12}$$

and so, for stability, we require

$$\left|\frac{\alpha^2}{4\left(1+\frac{\alpha^2}{4}\right)}\right| < 1 \tag{4.13}$$

i.e.

$$-4-\alpha^2 < \alpha^2 < 4+\alpha^2. \tag{4.14}$$

This will be satisfied for all real values of α, and hence the fixed point $\overline{x} = \frac{1}{2}$ will always be stable.

Two free nodes

As in the one free node case, the weight functions using the exact and the approximate derivatives are the same. The two free node grid is given by $x_0 = 0$, $x_1 = x_1$, $x_2 = x_2$, and $x_3 = 1$. Hence $x_{\frac{1}{2}} = \frac{x_1}{2}$, $x_{\frac{3}{2}} = \frac{x_2+x_1}{2}$, and $x_{\frac{5}{2}} = \frac{1+x_2}{2}$.

Now, using the exact derivative,

$$f'(x) = \alpha(1 - 2x) \tag{4.15}$$

the weight function given by Equation (1.2) is

$$\begin{aligned} w_{\frac{1}{2}} &= \sqrt{1 + \alpha^2(1 - x_1)^2}, \\ w_{\frac{3}{2}} &= \sqrt{1 + \alpha^2(1 - (x_1 + x_2))^2}, \qquad \text{and} \\ w_{\frac{5}{2}} &= \sqrt{1 + \alpha^2 x_2^2}. \end{aligned} \tag{4.16}$$

If we use the approximate derivative, as given in Equation (2.3), the weight functions are

$$\begin{aligned} w_{\frac{1}{2}} &= \sqrt{1 + \left(\tfrac{f(x_1) - f(x_0)}{x_1 - x_0}\right)^2} = \sqrt{1 + \alpha^2(1 - x_1)^2}, \\ w_{\frac{3}{2}} &= \sqrt{1 + \left(\tfrac{f(x_2) - f(x_1)}{x_2 - x_1}\right)^2} = \sqrt{1 + \left(\tfrac{\alpha x_2(1 - x_2) - \alpha x_1(1 - x_1)}{x_2 - x_1}\right)^2} \\ &= \sqrt{1 + \alpha^2(1 - x_2 - x_1)^2}, \qquad \text{and} \\ w_{\frac{5}{2}} &= \sqrt{1 + \left(\tfrac{f(x_3) - f(x_2)}{x_3 - x_2}\right)^2} = \sqrt{1 + \alpha^2 x_2^2}. \end{aligned} \tag{4.17}$$

Clearly, the weight functions are the same when using either the exact derivative or the approximate derivative.

Substituting the weight functions in Equation(2.4), we look for fixed points of x_1 and x_2 in the usual way, giving

$$\begin{aligned} &\sqrt{1 + \alpha^2(1 - (\overline{x}_1 + \overline{x}_2))^2}(\overline{x}_2 - \overline{x}_1) = \sqrt{1 + \alpha^2(1 - \overline{x}_1)^2}\overline{x}_1, \qquad \text{and} \\ &\sqrt{1 + \alpha^2\overline{x}_2^2}(1 - \overline{x}_2) = \sqrt{1 + \alpha^2(1 - (\overline{x}_1 + \overline{x}_2))^2}(\overline{x}_2 - \overline{x}_1). \end{aligned} \tag{4.18}$$

We look for fixed points of x_1 and x_2 in the usual way, by setting $x_1^n = x_1^{n+1} = \overline{x_1}$ and $x_2^n = x_2^{n+1} = \overline{x_2}$. In order to be able to solve these, we use the fact that the function $f(x)$ is symmetric, and assume symmetry of the resulting grid, i.e.

$$x_1 = 1 - x_2. \tag{4.19}$$

If we start with a symmetric grid, so that assumption (4.19) will certainly be true, then we can verify from (4.18) that it will still hold for the updated grid. We substitute $x_1^n = 1 - x_2^n$ in the two equations (4.18), and then solve simultaneously to find x_1^{n+1} in terms of x_2^{n+1}. We find that $x_1^{n+1} = 1 - x_2^{n+1}$, therefore, if starting with a symmetric grid, (4.19) is a valid assumption to make. However, if we start with a skewed grid, we cannot make this assumption, and it is not possible to find the fixed points, even using Mathematica.

Solving the second of these two equations, using the assumption, and looking for fixed points of x_2 we find 4 roots. The first one is $\overline{x}_2 = 0$. The second root is always less than 0.5, and the third root is always less than zero, for all values of α in the the range $[0.5, 50]$. A fixed point of x_2 must be in the region $[0.5, 1]$, so these three roots cannot be obtained using the tridiagonal iteration. The fourth root is in the region $[0.5, 1]$ for all values of α in the range, see Figure 4.5. This root is the only possible root when using the tridiagonal iteration. We now investigate the stability of this root. Figure 4.6 shows the derivative, with the root substituted, against α. As can be seen, $f'(x_4)$ is in the range $[0, 1]$, so this root is stable for all $\alpha \in [0.1, 50]$.

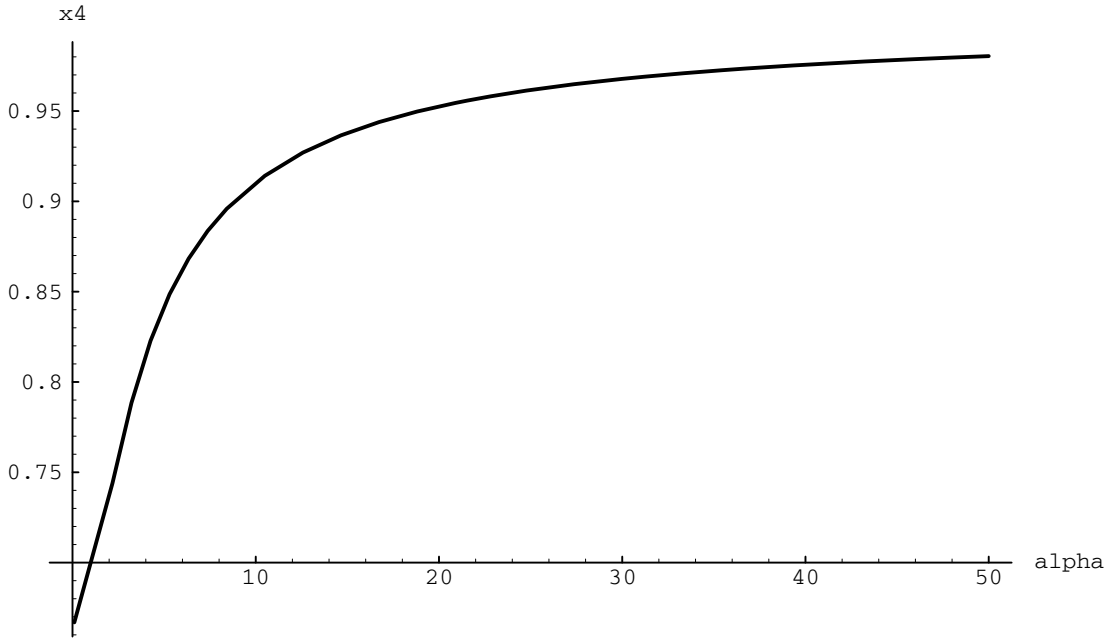

Figure 4.5: Analytic equidistribution solution for the node x_2, Tridiagonal iteration, quadratic function, 2 free nodes.

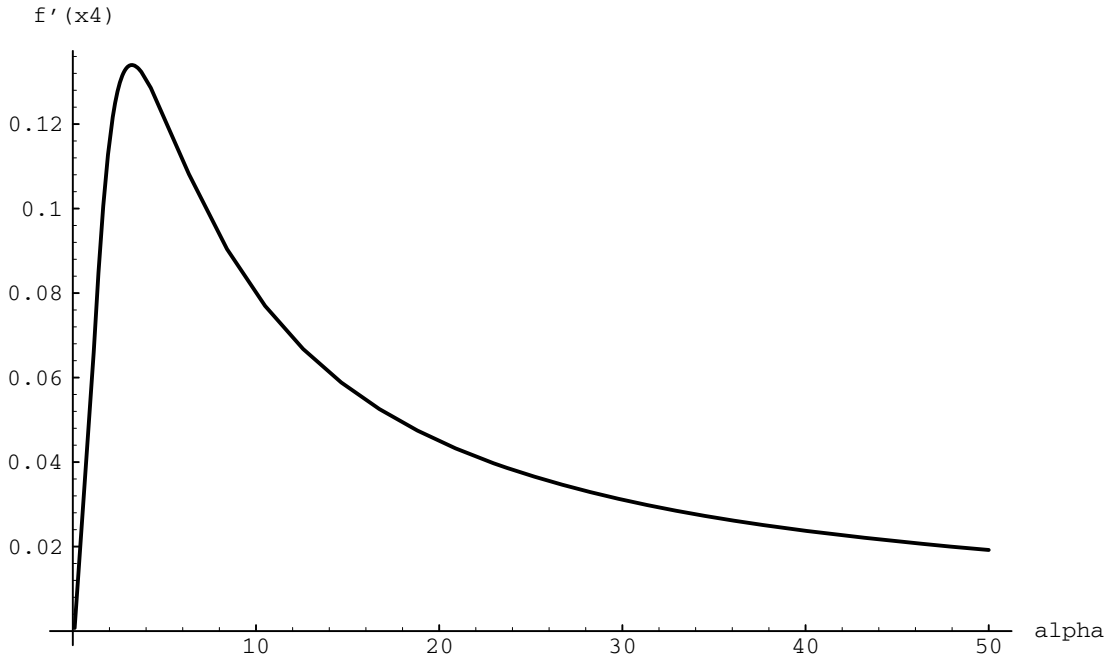

Figure 4.6: Analytic stability condition for the node x_2, Tridiagonal iteration, quadratic function, 2 free nodes.

4.3.2 Cubic Function : $f(x) = \alpha x(\frac{1}{2} - x)(1 - x)$

This time the weight functions using the exact and the approximate derivatives are not the same.

Exact derivative - One free node

Again, the one free node grid is given by $x_0 = 0$, $x_1 = X$ and $x_2 = 1$. Hence, $x_{\frac{1}{2}} = \frac{X}{2}$, and $x_{\frac{3}{2}} = \frac{1+X}{2}$, and using the exact derivative,

$$f'(x) = \frac{1}{2}\alpha - 3\alpha x + 3\alpha x^2, \tag{4.20}$$

the weight functions, using Equation (1.2), are

$$\begin{aligned} w_{\frac{1}{2}} &= \sqrt{1 + \alpha^2 \left(\tfrac{1}{2} - \tfrac{3X}{2} + \tfrac{3X^2}{2}\right)^2}, \qquad \text{and} \\ w_{\frac{3}{2}} &= \sqrt{1 + \alpha^2 \left(\tfrac{3X^2}{4} - \tfrac{1}{4}\right)^2}. \end{aligned} \tag{4.21}$$

Substituting the weight functions in Equation (2.4), we look for fixed points of the grid, giving :

$$\sqrt{1 + \alpha^2 \left(\frac{3\overline{x}^2}{4} - \frac{1}{4}\right)^2}(1 - \overline{x}) = \sqrt{1 + \alpha^2 \left(\frac{1}{2} - \frac{3\overline{x}}{2} + \frac{3\overline{x}^2}{2}\right)^2}\overline{x}, \tag{4.22}$$

and find, after squaring both sides and solving for $\overline{x}$ that there are five roots of Equation (4.22). The first two are complex and so cannot be attained. The third root is less than 0, and the fourth is greater than 1, so using the tridiagonal iteration, these fixed points will not be found. The last root is $\overline{x} = \frac{1}{2}$. This is the only feasible root when using the tridiagonal iteration, and we now examine its stability. We find that,

$$f'(\frac{1}{2}) = -\frac{3\alpha^2}{8\left(16 + \frac{\alpha^2}{16}\right)}, \tag{4.23}$$

and so, for stability, we require

$$\left|\frac{3\alpha^2}{8\left(16 + \frac{\alpha^2}{16}\right)}\right| < 1, \tag{4.24}$$

i.e.

$$-\frac{256}{5} < \alpha^2 < \frac{256}{5} = 51.2. \tag{4.25}$$

This is the inequality which α must satisfy for the root to be stable. When $\alpha^2 > 51.2$, the root $\overline{x} = \frac{1}{2}$ will be unstable.

Approximate derivative - One free node

As before, the grid is given by $x_0 = 0$, $x_1 = X$, and $x_2 = 1$. Using the approximate derivative as defined in Equation (2.3), the weight functions at the nodes are

$$\begin{aligned} w_{\frac{1}{2}} &= \sqrt{1 + (\tfrac{f(x_1)-f(x_0)}{x_1-x_0})^2} = \sqrt{1 + \alpha^2(\tfrac{1}{2} - \tfrac{3}{2}X + X^2)^2}, \qquad \text{and} \\ w_{\frac{3}{2}} &= \sqrt{1 + (\tfrac{f(x_2)-f(x_1)}{x_2-x_1})^2} = \sqrt{1 + \alpha^2 X^2(\tfrac{1}{2} - X)^2}, \end{aligned} \tag{4.26}$$

and substituting these in Equation (2.4), we look for fixed points $\overline{x}$,

$$\sqrt{1 + \alpha^2\overline{x}^2(\frac{1}{2} - \overline{x})^2}(1 - \overline{x}) = \sqrt{1 + \alpha^2(\frac{1}{2} - \frac{3}{2}\overline{x} + \overline{x}^2)^2}\overline{x}. \tag{4.27}$$

After squaring both sides of Equation (4.27), and then solving for $\overline{x}$, we find that the only fixed point is $\overline{x} = \frac{1}{2}$. We then solve Equation (4.27) for x^{n+1}, find the derivative, and substitute in the root $\overline{x} = \frac{1}{2}$. We find

$$f'(\frac{1}{2}) = 0, \tag{4.28}$$

which clearly this satisfies the stability criterion, and so the fixed point will be unconditionally stable.

Two free nodes

We find, for the case of two free nodes, that the weight functions are not the same using the exact and the approximate derivatives. However, in each case

the equations found from (2.4) are too complicated to solve, even when assuming symmetry, and using Mathematica. (see Subsection 4.3.1 using two free nodes.)

4.3.3 Tridiagonal Iteration - Results

We find that, in general, the results obtained for the quadratic and cubic functions with 1 or 2 free nodes are as predicted by the analysis. The most notable exception is the quadratic function, with 1 free node and the exact derivative. We expect from analysis a stable fixed point at $x = \frac{1}{2}$, but this is not the result we get, see Figure 4.7. From approximately $\alpha = 13$, the equidistribution solution moves away from $x = 0.5$, to the left, and is also not quite converged. We find that if we start with a grid skewed to the right, the solution moves in the opposite direction, also to the right. A uniform initial grid however remains at the fixed

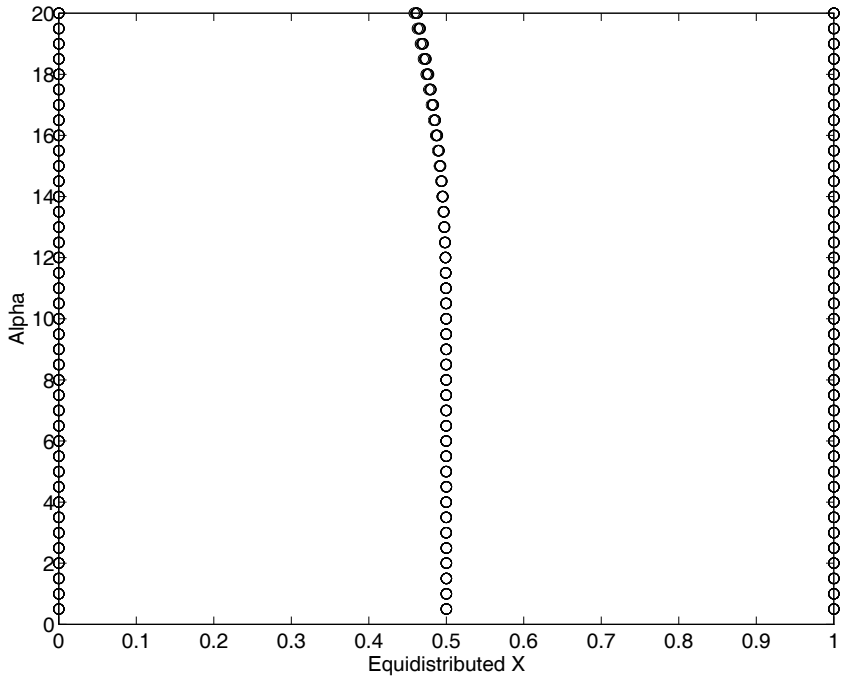

Figure 4.7: Last 10 nodal positions for the Tridiagonal iteration, quadratic function, exact derivative, 1 free node.

point $x = \frac{1}{2}$. We do not know the precise reason for this, and both program and analysis appear correct. There is a possibility that the dependence on the initial grid, and the slight hint of a period 2 nature to the deviation from $x = \frac{1}{2}$, means that there are stable period 2 solutions of the equations.

The quadratic function with two free nodes gives the results predicted by analysis. However, the predicted results do not agree with the "exact" nodal placements obtained by fine quadrature equidistribution, as described in Section 2.4. It appears that the tridiagonal iteration, by its definition, will not give correct equidistribution results for the quadratic function with two free nodes. This however should not be too surprising since the derivation of the tridiagonal iteration involves an approximation to the original equidistribution, with the error being potentially large for large nodal spacing. For 11 and 12 free points, with both the exact and the approximate derivatives, the quadratic function converges correctly. As expected, the cubic function with one free node and using the exact derivative, converged for $\alpha < 7.1$. Above this value of α we get a period 2 solution, again, as expected.

The cubic function with two free nodes gives very similar results for the exact and the approximate derivatives for $\alpha \leq 8.5$. With the exact derivative, the solution trajectories are smooth at $\alpha \approx 8.5$, whereas, with the approximate derivative, the solution appears to bifurcate to a spurious steady state (see Figure 4.9, with the "exact" solution in Figure 4.8). Both cases have period 2 solutions in the region, approximately, $15 \leq \alpha \leq 18$, and are unconverged for $\alpha > 18$.

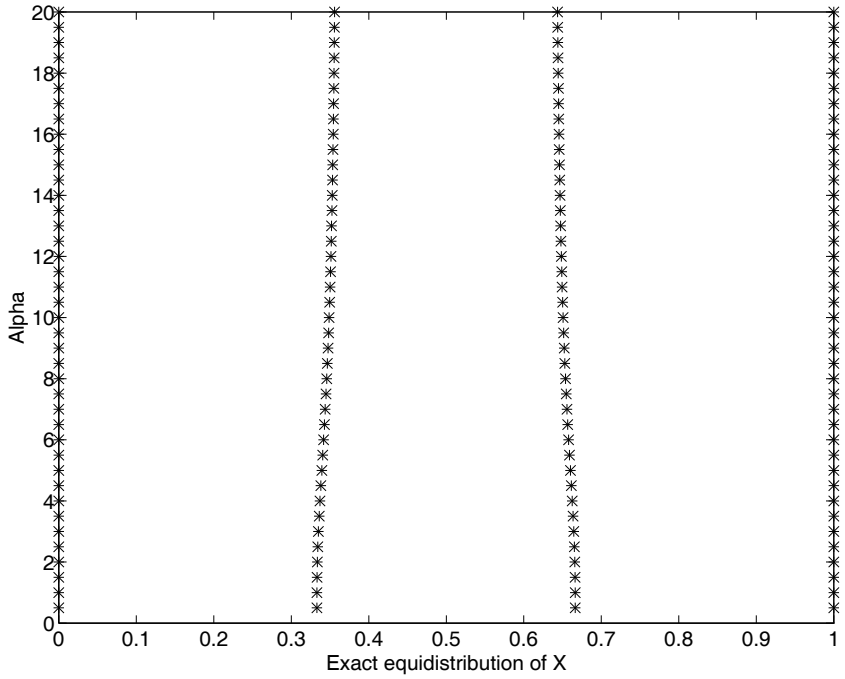

Figure 4.8: "Exact" nodal positions, using fine quadrature, for the cubic function, 2 free nodes.

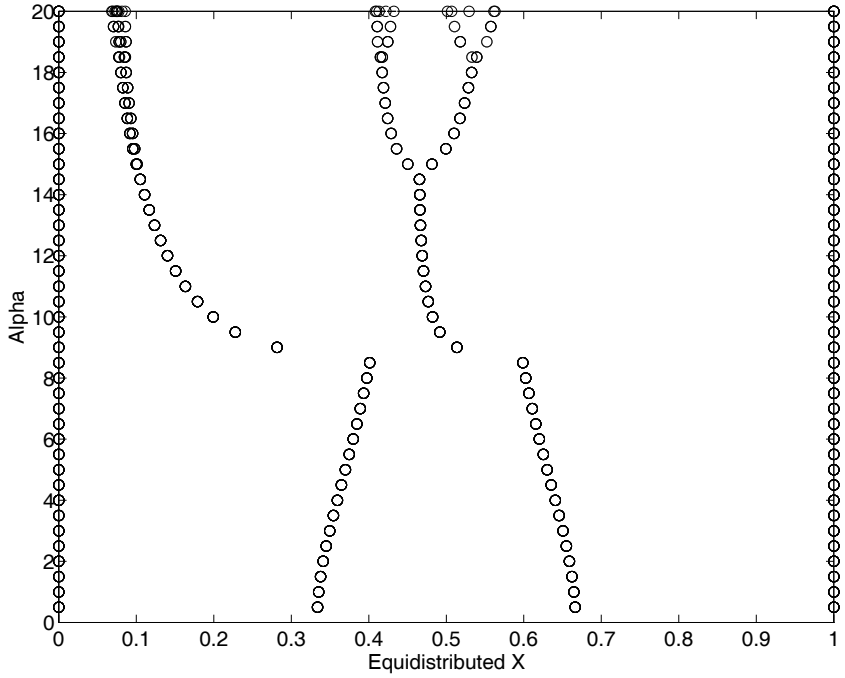

Figure 4.9: Last 10 nodal positions for the Tridiagonal iteration, cubic function, approximate derivative, 2 free nodes.

With 11 and 12 free nodes, using the exact and the approximate derivatives, the cubic function appears to converge to a spurious solution (incorrect when compared to the "exact" nodal placements.) In Figure 4.11, with 11 free points, this solution bifurcates with what appears to be a transcritical bifurcation (see [6]), before becoming unstable at, either $\alpha = 42$ for the approximate derivative, or $\alpha = 23$ for the exact derivative (see Figure 4.10 for the "exact" solution). With 12 free points, the solution becomes period 2 and then is unconverged, but, again, the is incorrect when compared with the "exact" solution.

We looked at some plots of the Condition number of the tridiagonal matrix against α. However, these gave no useful information about the cause of the dynamics of the solutions.

The solution for the exponential function is not dependent on whether there is an even or an odd number of free nodes and the equidistribution solution converges correctly when the approximate derivative is used. Using the exact derivative, the solutions for both the exponential and the tanh functions behave the same way. The solution converges for all values of α in the range used, but the solution is only correct for $\alpha \geq 10^{-1.7}$. Below this, the solution trajectories are parallel and equally spaced. Using the approximate derivative, with the tanh function, the results converge correctly for a greater range of α using 12 free nodes than 11 free nodes. With 12 free nodes, the solution is correctly converged for $\alpha \geq 10^{-1.9}$, and below this the solution is totally unconverged or period 2. With 11 free nodes, the solution is only converged correctly for $\alpha \geq 10^{-1.4}$. Below this, $10^{-2.2} \leq \alpha < 10^{-1.4}$ it is unconverged, and for $\alpha < 10^{-2.2}$, the solution has converged incorrectly into equally spaced parallel tracks.

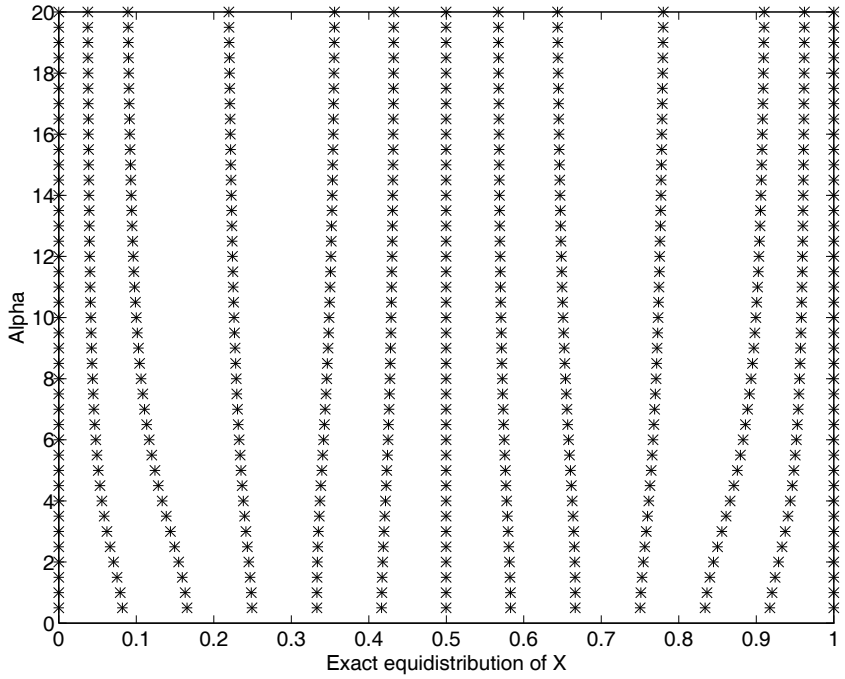

Figure 4.10: "Exact" nodal positions, using fine quadrature, for the cubic function, 11 free nodes.

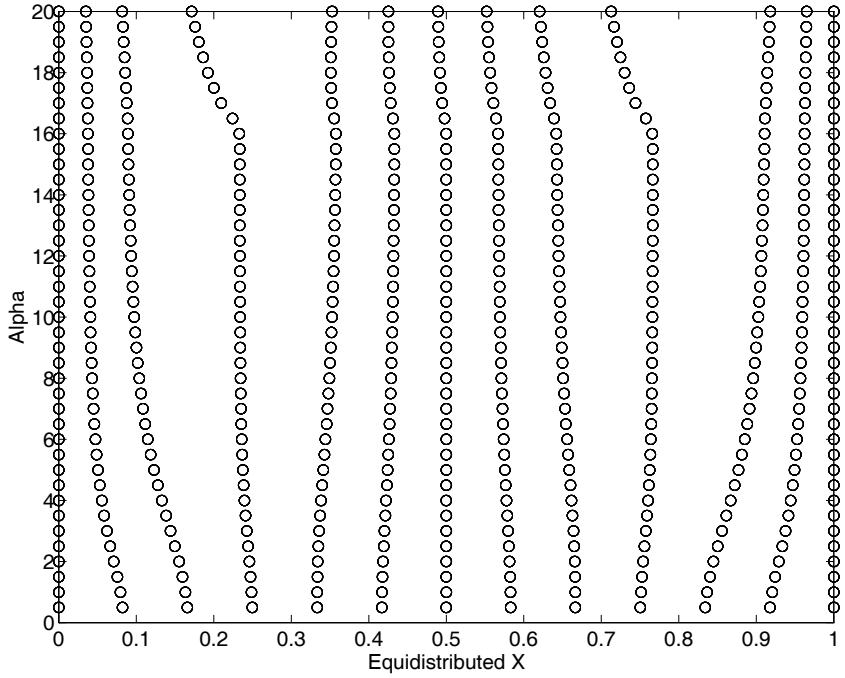

Figure 4.11: Last 10 nodal positions for the Tridiagonal iteration, cubic function, approximate derivative, 11 free nodes.

4.4 Ren and Russell Iteration - Analysis

We consider, for analysis, the case of one free node, and investigate both the cases where the exact derivative is used, and where the approximate derivative is used.

4.4.1 Quadratic function : $f(x) = \alpha x(1-x)$

One free node - Approximate derivative

As with the tridiagonal iteration, the one free node grid is given by $x_0 = 0$, $x_1 = X$, and $x_2 = 1$. Hence, using Equation (2.26), the weight functions are

$$\begin{aligned} w_0 &= \sqrt{1 + \left(\tfrac{f(x_1)-f(x_0)}{x_1-x_0}\right)^2} = \sqrt{1+\alpha^2(1-X)^2}, \qquad \text{and} \\ w_1 &= \sqrt{1 + \left(\tfrac{f(x_2)-f(x_1)}{x_2-x_1}\right)^2} = \sqrt{1+\alpha^2X^2}. \end{aligned} \tag{4.29}$$

Now, substituting these into Equation (2.23), we get

$$-2\Delta t\dot{X}\sqrt{1+\alpha^2(1-X^n)^2} = \sqrt{1+\alpha^2(1-X^n)^2}X^n - \sqrt{1+\alpha^2(X^n)^2}(1-X^n), \tag{4.30}$$

and using Equation (2.27), we substitute for $\dot{X}$ to obtain

$$\begin{aligned} -2(X^{n+1}-X^n)\sqrt{1+\alpha^2(1-X^n)^2} = \\ \sqrt{1+\alpha^2(1-X^n)^2}X^n - \sqrt{1+\alpha^2(X^n)^2}(1-X^n). \end{aligned} \tag{4.31}$$

We now look for fixed points, by putting $\overline{x} = X^n = X^{n+1}$. Hence, the left-hand side of Equation (4.31) is equal to zero and the resulting equation is the same as for the tridiagonal iteration and the quadratic function, see Section 4.3.1. Therefore, as found in that analysis, there is one fixed point $\overline{x} = \frac{1}{2}$. However, we would not expect the stability analysis to be the same. We find that

$$f'(\frac{1}{2}) = \frac{\alpha^2}{4\left(1+\frac{\alpha^2}{4}\right)}, \tag{4.32}$$

so, for stability we require

$$\left| \frac{\alpha^2}{4\left(1+\frac{\alpha^2}{4}\right)} \right| < 1, \tag{4.33}$$

i.e.

$$-4-\alpha^2 < \alpha^2 < \alpha^2+4. \tag{4.34}$$

Clearly, the fixed point is unconditionally stable.

This is the same stability condition as was found for the tridiagonal iteration and the quadratic function, for the fixed point $\overline{x} = \frac{1}{2}$. The derivatives, $f'(x^n)$, are not the same from these two cases, but when the fixed point $\overline{x} = \frac{1}{2}$ is substituted, the two cases give identical results.

One free node - Exact derivative

With the one free node grid, $x_0 = 0$, $x_1 = X$, $x_2 = 1$, we get, from Equation (2.24) using the exact derivative, $f'(x) = \alpha(1-2x)$,

$$\begin{aligned} w_0 &= \sqrt{1+\alpha^2}, \qquad \text{and} \\ w_1 &= \sqrt{1+\alpha^2(1-2X)^2}. \end{aligned} \tag{4.35}$$

Substituting these into Equation(2.23), gives

$$-2\Delta t\dot{X}\sqrt{1+\alpha^2} = \sqrt{1+\alpha^2}X^n - \sqrt{1+\alpha^2(1-2X^n)^2}(1-X^n), \tag{4.36}$$

and using Equation (2.27), we substitute for $\dot{X}$, and get

$$-2(X^{n+1}-X^n)\sqrt{1+\alpha^2} = \sqrt{1+\alpha^2}X^n - \sqrt{1+\alpha^2(1-2X^n)^2}(1-X^n). \tag{4.37}$$

Looking for the steady states of this equation, we find four roots. The first two are complex and so cannot be attained. The next root is always greater than 1, and if attained would cause grid tangling. The last root is in the region $[0,1]$,

see Figure 4.12. We investigate its stability in the usual way and find that it is always stable for α in the range $[0.1, 50]$ (see Figure 4.13).

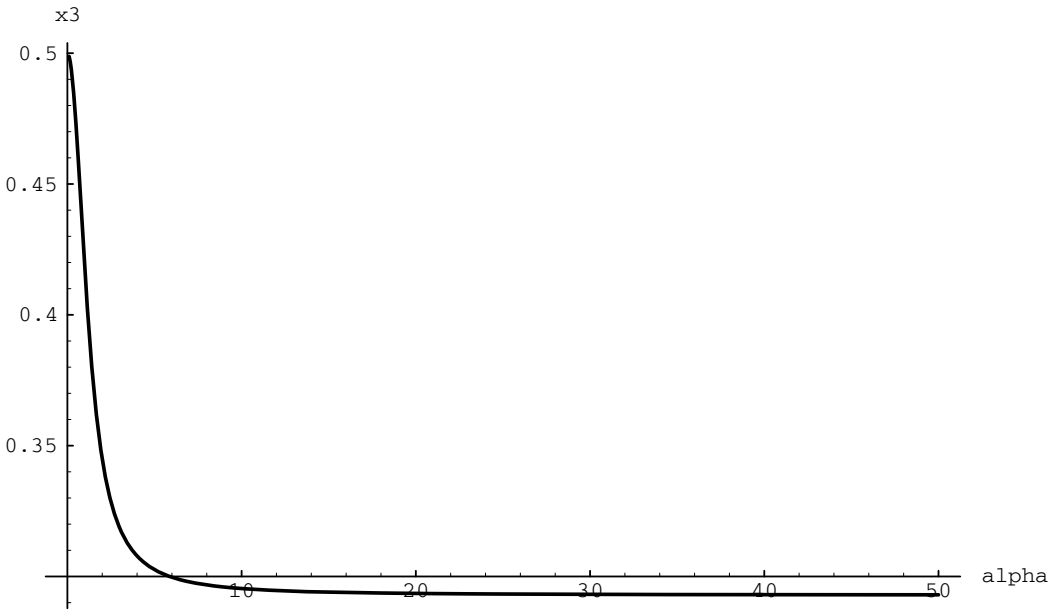

Figure 4.12: Analytic equidistribution solution for the Ren and Russell iteration, quadratic function, exact derivative, 1 free node.

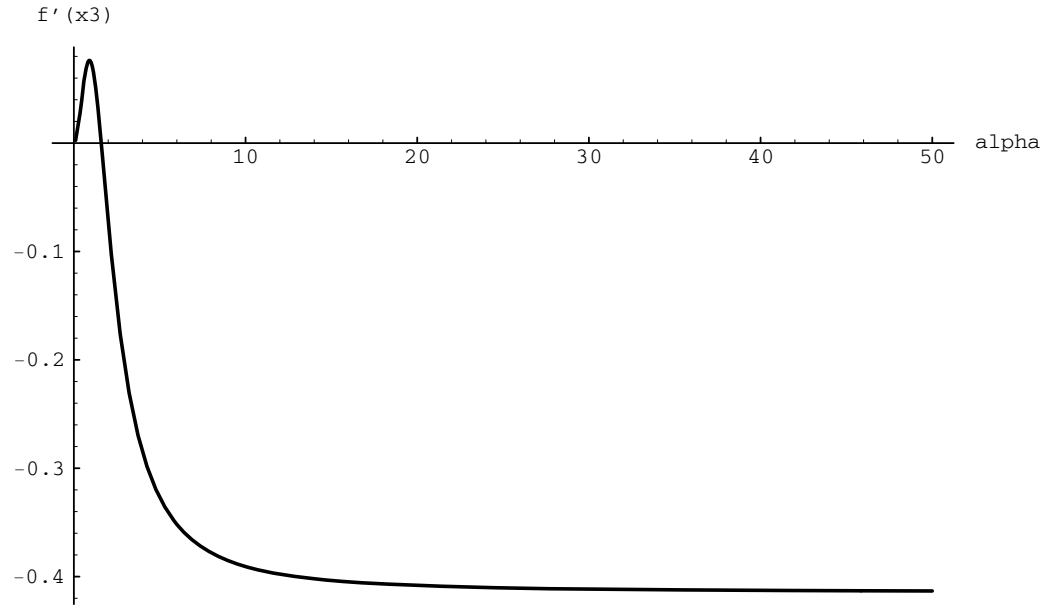

Figure 4.13: Analytic stability condition for the Ren and Russell iteration, quadratic function, exact derivative, 1 free node.

4.4.2 Cubic Function : $f(x) = \alpha x(\frac{1}{2} - x)(1 - x)$

One free node - Approximate derivative

Using the grid $x_0 = 0$, $x_1 = X$, $x_2 = 1$, and using Equation (2.26) for w, we find

$$\begin{aligned} w_0 &= \sqrt{1 + \left(\tfrac{f(x_1)-f(x_0)}{x_1-x_0}\right)^2} = \sqrt{1 + \alpha^2((\tfrac{1}{2} - X)(1 - X))^2}, \qquad \text{and} \\ w_1 &= \sqrt{1 + \left(\tfrac{f(x_2)-f(x_1)}{x_2-x_1}\right)^2} = \sqrt{1 + \alpha^2 X^2(\tfrac{1}{2} - X)^2}. \end{aligned} \tag{4.38}$$

Substituting into Equation (2.23), and replacing $\dot{X}$ using Equation (2.27), yields

$$\begin{aligned} -2(X^{n+1} - X^n)\sqrt{1 + \alpha^2((\tfrac{1}{2} - X^n)(1 - X^n))^2} = \\ \sqrt{1 + \alpha^2((\tfrac{1}{2} - X^n)(1 - X^n))^2}X^n - \sqrt{1 + \alpha^2(X^n)^2(\tfrac{1}{2} - X^n)^2}(1 - X^n). \end{aligned} \tag{4.39}$$

We look for fixed points in the usual way, by replacing $\overline{x} = X^n = X^{n+1}$, and the left-hand side of Equation (4.39) becomes equal to zero. The resulting equation is the same as for the tridiagonal iteration and the cubic function, (Subsection 4.3.2), using the approximate derivative. So, as for that case, the only fixed point is $\overline{x} = \frac{1}{2}$.

Performing the stability analysis we find that

$$f'(\frac{1}{2}) = 0, \tag{4.40}$$

so the fixed point is unconditionally stable.

Again, although the derivatives $f'(x^n)$ are not the same for the two cases, when the fixed point is substituted the results are identical.

One free node - Exact derivative

The equations for this case are too complicated to solve.

4.5 Ren and Russell Iteration - Results

As has been shown in the analysis, when the Euler equation (2.27) is substituted in Equation (2.23), the Δt term will cancel out.

We find that, with one exception, the results obtained for the quadratic and cubic functions with one free node, behave as predicted by the analysis. The exception is the quadratic function using an approximate derivative. This behaves in the same unexplained way as the tridiagonal iteration and the quadratic function using the exact derivative. (see Figure 4.7 in Section 4.3.3) As in that case, if the starting grid is skewed the other way, the equidistribution solution moves in that direction, and if a symmetric starting grid is used, the solution stays at $x = \frac{1}{2}$. Clearly, the behaviour is dependent on the starting grid.

Using the exact derivative, we find for both the quadratic and cubic functions, using an odd and an even number of free nodes, that the method breaks down when α reaches approximately 23. This is due to the matrix becoming singular, (this is the matrix holding the values on the right-hand side of Equation (2.23)). A plot of the condition number of the matrix against α shows the condition number steadily increasing an α increases.

Using the approximate derivative, the quadratic function with 11 free nodes converged in the range $\alpha \in [0.5, 20]$, although the results did not agree with the "exact" nodal placements, probably due to the approximation errors in the derivation of the iteration. However, with 12 free nodes, convergence was only obtained for $\alpha < 8$, again incorrectly. Above this, the solution was period 2, and then was unconverged.

The cubic function using the approximate derivative and 11 free nodes appears

to have a transcritical bifurcation at $\alpha = 16.5$, see Figure 4.14 (again Figure 4.10 shows the "exact" solution), since the solution remains unchanged if the starting grid is skewed the other way. With 12 free nodes, convergence is obtained for $\alpha < 16$, but is unconverged above.

As expected, the results with the exponential function are not significantly different if there is an odd or an even number of free nodes. Using the exact derivative the solution converges correctly for $\alpha \geq 10^{-1.1}$. For $10^{-1.8} < \alpha < 10^{-1.1}$, the solution is unconverged, and for $\alpha \leq 10^{-1.8}$ the solution converges incorrectly into equally spaced parallel tracks. With the approximate derivative, the method will not work for $\alpha \leq 10^{-1.9}$, due to the matrix becoming singular. For α greater than this, the solution converged correctly.

For the tanh function using the approximate derivative, there is not a great difference between the results for 11 and 12 free nodes. The solution converged correctly for approximately $\alpha \geq 10^{-2}$, and below this the solution is unconverged or there is a period 2 solution. In this region, x takes values in the range $[-1, 2.5]$. Using the exact derivative, there is again not much difference between 11 and 12 free nodes in both cases the solution has converged correctly for approximately $\alpha \geq 10^{-0.9}$, and in the region $10^{-2.2} \leq \alpha \leq 10^{-1.2}$, is unconverged. With 11 free nodes, for $\alpha < 10^{-2.2}$, there is a period 2 solution. With 12 free nodes and $\alpha < 10^{-2.2}$ the solution has converged into equally spaced parallel tracks.

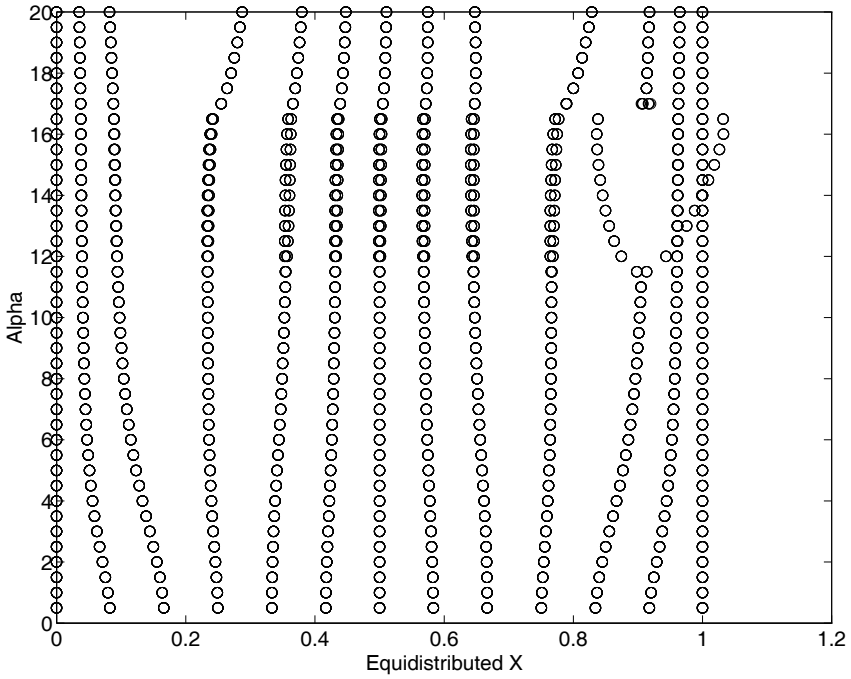

Figure 4.14: Last 10 nodal positions for the Ren and Russell iteration, cubic function, approximate derivative, 11 free nodes.

4.6 Nominal Iteration - Analysis

For analysis, we look at the case of one free node, and we consider only the case where the exact derivative is used.

4.6.1 Quadratic Function - $f(x) = \alpha x(1-x)$

We use, as before, the one free node grid of $x_0 = 0$, $x_1 = X$, $x_2 = 1$. Then we use the exact first derivative

$$f'(x) = \alpha(1-2x), \tag{4.41}$$

and the exact second derivative

$$f''(x) = -2\alpha, \tag{4.42}$$

and substitute into Equation (2.37). Note that, with one free node, $\xi = \frac{1}{2}$. So,

$$-\frac{2X^{n+1}+1}{(\frac{1}{2})^2} + \left(\frac{\alpha(1-2X^n)(-2\alpha)}{1+\alpha^2(1-2X^n)^2}\frac{1}{2\frac{1}{2}}\right)\frac{1}{2\frac{1}{2}} = 0, \tag{4.43}$$

i.e.

$$4(1-2X^{n+1}) + \left(\frac{-2\alpha^2(1-2X^n)}{1+\alpha^2(1-2X^n)^2}\right) = 0, \tag{4.44}$$

or

$$4 - 8X^{n+1} = \frac{2(1-2X^n)}{\frac{1}{\alpha^2}+(1-2X^n)^2}. \tag{4.45}$$

To find the steady state, we let $\overline{x} = X^n = X^{n+1}$, yielding

$$4(1-2\overline{x}) = \frac{2(1-2\overline{x})}{\frac{1}{\alpha^2}+(1-2\overline{x})^2}. \tag{4.46}$$

This has roots $\overline{x} = \frac{1}{2}$, and $\overline{x} = \frac{1}{2} \pm \frac{1}{2}\sqrt{\frac{1}{2} - \frac{1}{\alpha^2}}$. If $\alpha^2 \leq 2$ then the only real fixed point is $\overline{x} = \frac{1}{2}$, if $\alpha^2 > 2$, then $\overline{x} = \frac{1}{2}$ is a triple root. We now investigate the stability of each steady state.

We find that

$$f'(\frac{1}{2}) = \frac{\alpha^2}{2}, \tag{4.47}$$

and so for stability we require

$$\left|\frac{\alpha^2}{2}\right| < 1, \tag{4.48}$$

i.e.

$$\alpha^2 < 2. \tag{4.49}$$

Hence the fixed point $\overline{x} = \frac{1}{2}$ will be stable for $\alpha^2 < 2$, and will be unstable elsewhere.

For the other two roots, their stability conditions are identical, see Figure 4.15 for a plot of the derivative with one of the roots substituted against α. The derivative becomes equal to one at $\alpha = \sqrt{2}$, so these two fixed points are stable for $\alpha > \sqrt{2}$.

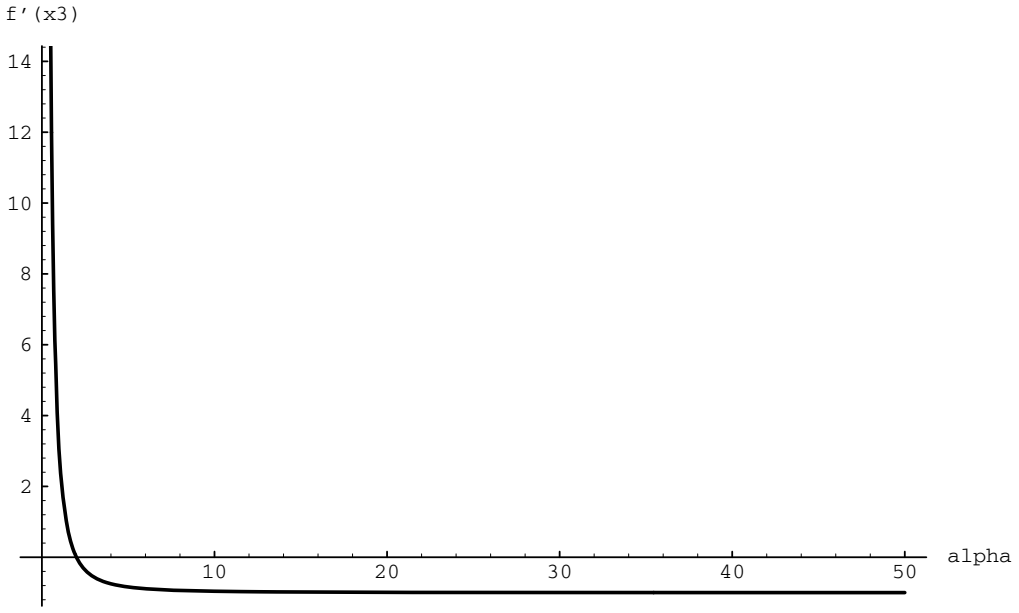

Figure 4.15: Analytic stability condition for the Nominal iteration, quadratic function, exact derivative, 1 free node.

4.6.2 Cubic Function : $f(x) = \alpha x(\frac{1}{2} - x)(1 - x)$

We use the one free node grid $x_0 = 0$, $x_1 = X$, $x_2 = 1$, and the exact first and second derivatives

$$f'(x) = \frac{1}{2}\alpha - 3\alpha x + 3\alpha x^2, \tag{4.50}$$

and

$$f''(x) = -3\alpha + 6\alpha x \tag{4.51}$$

Substituting in Equation (2.37), with $\xi = \frac{1}{2}$, yields

$$4(1 - 2X^{n+1}) + \frac{(\frac{1}{2}\alpha - 3\alpha X^n + 3\alpha(X^n)^2)(-3\alpha + 6\alpha X^n)}{1 + (\frac{1}{2}\alpha - 3\alpha X^n + 3\alpha(X^n)^2)^2} = 0. \tag{4.52}$$

To find steady states, we set $\overline{x} = X^n = X^{n+1}$, and solve. The fixed points found are $\overline{x} = \frac{1}{2}$ and four other roots,

$$x_2, x_3 = \frac{1}{2} \pm \sqrt{10 - 2\sqrt{\frac{64}{\alpha^2} + 9}}, \tag{4.53}$$

and

$$x_4, x_5 = \frac{1}{2} \pm \sqrt{10 + 2\sqrt{\frac{64}{\alpha^2} + 9}}. \tag{4.54}$$

These roots will only be real for $\alpha > \sqrt{2}$

Stability analysis for the fixed point $\overline{x} = \frac{1}{2}$ gives the stability condition

$$\left|\frac{3\alpha^2}{16 + \alpha^2}\right| < 1, \tag{4.55}$$

i.e.

$$\alpha^2 < 8 \tag{4.56}$$

For the fixed points x_2 and x_3, their stability analysis is exactly the same. Figure 4.16 shows the derivative, with x_2 substituted, against α. We find that $f'(x_2) = -1$ at $\alpha = \frac{32+32\sqrt{10}}{3} \approx 3.85$, so these two fixed points are stable and real for

$$\frac{8}{3} \leq \alpha < 3.85. \tag{4.57}$$

The fixed points x_4 and x_5 are unstable for all α where the roots are real.

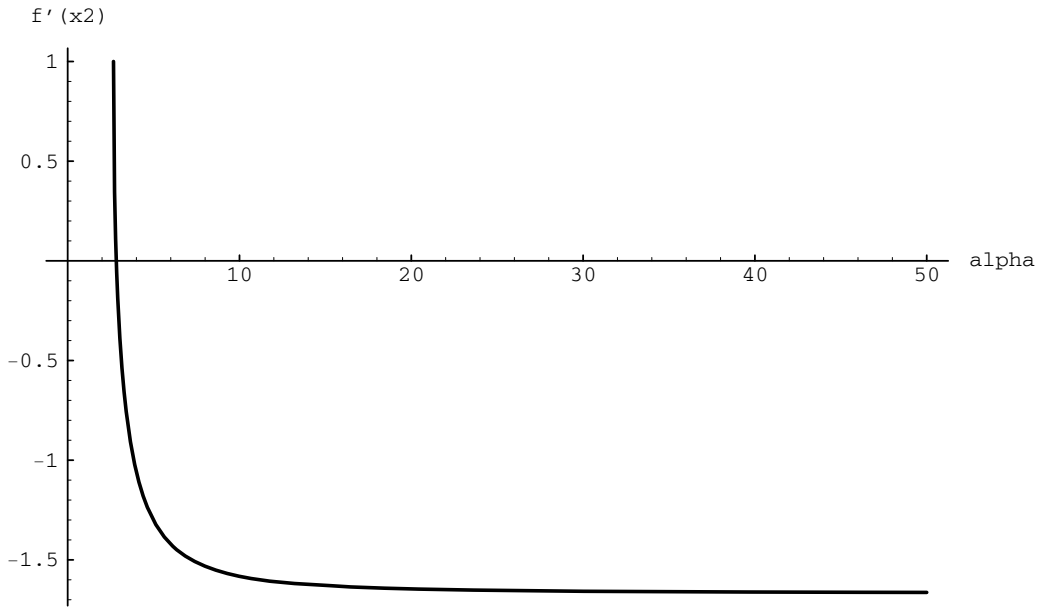

Figure 4.16: Analytic stability condition for the Nominal iteration, cubic function, exact derivative, 1 free node.

4.7 Nominal Iteration - Results

We only implement the nominal iteration with the exact derivative. We find that with one free node the results are as predicted by analysis. With the quadratic function, the equidistribution solution for $\alpha < \sqrt{2}$ is $x = \frac{1}{2}$. At $\alpha = \sqrt{2}$ there is a pitchfork bifurcation where there are two stable steady states, and an unstable steady state between them. Which of the two stable states is obtained depends on the starting grid.

We note that the results for all the functions were very similar for both an odd and an even number of free nodes.

The quadratic function converged incorrectly for $\alpha \leq 4.2$, but is unconverged for $\alpha > 4.2$.

The cubic function converged incorrectly for $\alpha < 2$. Then, as α increased, it had a period 2 solution, and then was unconverged. It converged again for $3.7 \leq \alpha \leq 4.2$. See Figure 4.17.

The exponential function appears to converge correctly for $\alpha \geq 10^{-0.4}$. For $10^{-2} \leq \alpha \leq 10^{-0.5}$, the solution is unconverged and for $\alpha < 10^{-2}$ the solution has converged into equally spaced parallel tracks.

The tanh function shows convergence and unconvergence in the same pattern as the exponential function. The main difference is that for $\alpha \geq 10^{-0.6}$ the solution has converged incorrectly.

It appears that the nominal iteration, as an equidistribution technique, behaves very poorly. For many values of α it does not converge, and when it does it is usually incorrect when compared with the "exact" nodal placements.

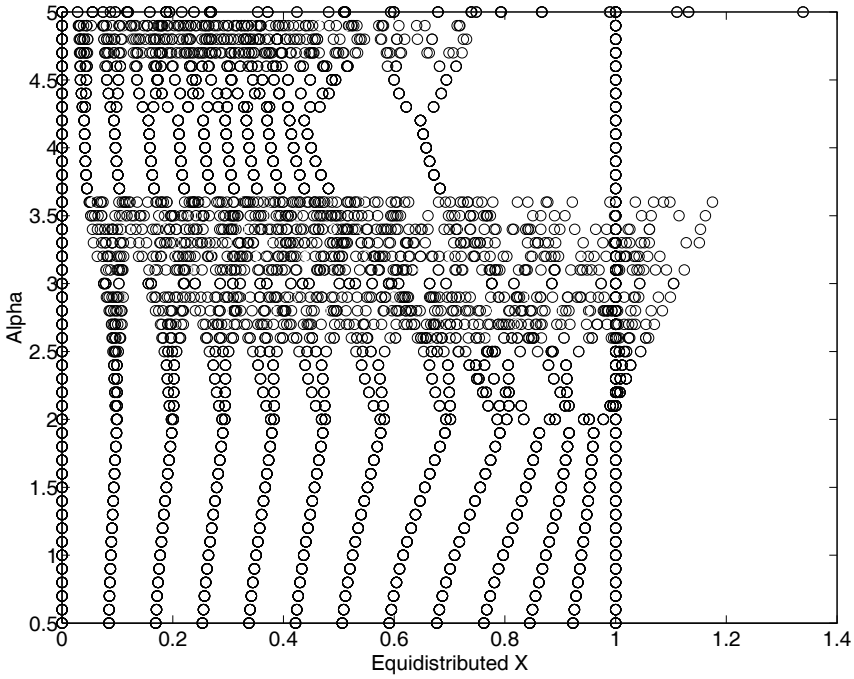

Figure 4.17: Last 10 nodal positions for the Nominal iteration, cubic function, exact derivative, 11 free nodes.

Chapter 5

PDE Solution with Grid Adaption

5.1 Test Problems

The test problems used in this section are the linear form of the convection-diffusion equation

$$u_t + u_x = \epsilon u_{xx} \tag{5.1}$$

with boundary conditions $u(0,t) = 0$, and $u(1,t) = 1$.

and the viscous Burger's equation

$$u_t + (\frac{1}{2}u^2)_x = \epsilon u_{xx} \tag{5.2}$$

with boundary conditions $u(0,t) = -1$, and $u(1,t) = -1$.

The steady state solutions are, for the linear case, the exponential function, and for the non-linear case, the tanh function (see Section 4.1). ϵ is substituted for α in these functions.

Following along the lines of [5], we use a method of lines approach to solve the PDE with central spatial differences,

$$u_{xx}|_j = \frac{\frac{u_{j+1}-u_j}{x_{j+1}-x_j} - \frac{u_j-u_{j-1}}{x_j-x_{j-1}}}{\frac{1}{2}(x_{j+1}-x_j)}, \tag{5.3}$$

and either upwind,

$$u_x|_j = \frac{f(u)_j - f(u)_{j-1}}{x_j - x_{j-1}}, \tag{5.4}$$

or central differences

$$u_x|_j = \frac{f(u)_{j+1} - f(u)_{j-1}}{x_{j+1} - x_{j-1}}, \tag{5.5}$$

for the convective term. The resulting system of ordinary differential equations (ODEs) for $\frac{du_k}{dt}$ is then solved using linearised implicit (backward) Euler, due to the small grid sizes that will occur, which would severely restrict time-steps for explicit methods.

The equation for implicit Euler is

$$\boldsymbol{u}^{n+1} = \boldsymbol{u}^n + \Delta t F(\boldsymbol{u}^{n+1}), \tag{5.6}$$

where $\dot{\boldsymbol{u}} = F(\boldsymbol{u})$, which is then linearised to give

$$\boldsymbol{u}^{n+1} = \boldsymbol{u}^n + \Delta t(F(\boldsymbol{u}^n) + J(\boldsymbol{u}^n)(\boldsymbol{u}^{n+1} - \boldsymbol{u}^n) + \ldots) \tag{5.7}$$

where $J(\boldsymbol{u}^n) = \frac{\partial F}{\partial u}$.

Neglecting higher order terms, we get

$$(I - \Delta t J(\boldsymbol{u}^n))\boldsymbol{u}^{n+1} = (I - \Delta t J(\boldsymbol{u}^n))\boldsymbol{u}^n + \Delta t F(\boldsymbol{u}^n), \tag{5.8}$$

which can be rewritten as

$$\boldsymbol{u}^{n+1} = \boldsymbol{u}^n + \Delta t(I - \Delta t J(\boldsymbol{u}^n))^{-1} F(\boldsymbol{u}^n). \tag{5.9}$$

Whilst the linearization is likely to degrade time accuracy it is expected to be suitable for steady-state calculations.

The regridding strategy adapted was to apply the grid adaption after every time step of the PDE method, either correcting the u_k after grid movement via interpolation from the old grid values, or performing no adjustment at all due to grid movement. We time-march to the steady state numerical solution, so the interpolation can be very crude. If we do not interpolate, we are in effect presenting new initial data for the PDE problem at each step.

Values of ϵ are looked at in the range $\epsilon \in [0.0001, 1]$. We iterate the discretised PDE and the grid adaption scheme for 200 steps, to allow the solution to reach an asymptotic steady state. If the solution is unconverged for all values of α, we run the method again using 400 steps.

Since we found in the previous section that there are few significant differences between the results for the exponential and tanh functions with 11 free nodes and the results with 12 free nodes, we use 11 free nodes only.

For the linear problem, since it has an unsymmetric steady state solution, we always use a skewed starting grid. For the non-linear problem, which has a symmetric steady state solution, both a skew and a symmetric starting grid are used.

We use two of the regridding techniques already described - the tridiagonal iteration, and the Ren and Russell iteration. Four different time-steps are used, $\Delta t = 1$, $\Delta t = 0.1$, $\Delta t = 0.01$, and $\Delta t = 0.001$.

We looked also at bifurcation diagrams of the l_2 norm of the solution against the log of ϵ. However, these did not reveal any more about dynamics of the

solutions, and so are not included here.

5.2 Results - Linear Problem

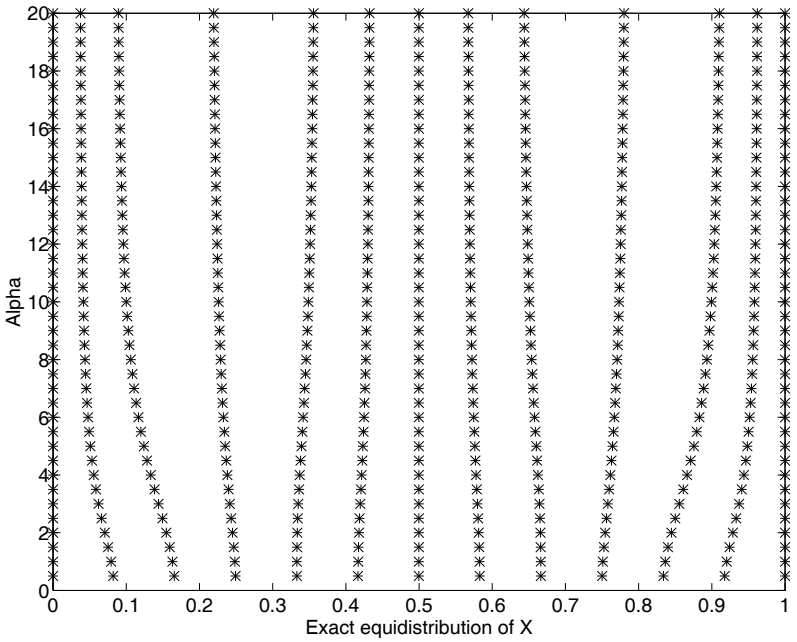

Figure 5.1: "Exact" nodal positions, using fine quadrature, of the steady state solution of the linear problem.

5.2.1 Tridiagonal Iteration

For all cases, when $\Delta t = 0.001$ the solution was not quite converged, and it appeared that if it had converged the solution would be incorrect, see Figure 5.2. For this reason, all of the rest of the results in this subsection are with $\Delta t = 1$, $\Delta t = 0.1$, and $\Delta t = 0.01$. Using central differences for the convective term, and both with and without interpolation, the method performs better as Δt decreases. For $\Delta t = 1$, the solution only converges for $\alpha \geq 10^{-2.2}$ (see Figure 5.3), whereas for $\Delta t = 0.01$ the solution converges correctly for all values of α.

Using the upwind scheme for the convective term, both with and without

interpolation, the solution converges correctly for all three values of Δt.

5.2.2 Ren and Russell Iteration

Again, for all cases when $\Delta t = 0.001$, the solution was not quite converged and did not appear correct, similar to Figure 5.2 with the tridiagonal iteration. Hence, the following results are all for $\Delta t = 1$, $\Delta t = 0.1$, and$\Delta t = 0.01$.

Using central differences for the convective term, and no interpolation, the method improves as Δt becomes smaller. As Δt decreases the range in which the solution has converged correctly also increases. unconverged, also decreases. The best result is for $\Delta t = 0.01$, where the solution has converged for $\alpha \geq 10^{-1.8}$.

Using central differences and performing interpolation, again, the range in which the solution has converged increases as Δt decreases. There are also some period 2 solutions with $\Delta t = 0.1$ and $\Delta t = 0.01$. See Figure 5.4 with $\Delta t = 0.01$, where there are period 2 solutions for $10^{-2.2} \leq \alpha \leq 10^{-1.5}$, and correct convergence above.

Using the upwind scheme for the convective term and no interpolation, the method converges correctly for a greater range of α as Δt decreases. With $\Delta t = 1$ and $dt = 0.1$, there are period 2 solutions in the unconverged region. Figure 5.5 is with $\Delta t = 0.1$ where the solution is period 2 for $\alpha \leq 10^{-2.6}$, either unconverged or period 2 for $10^{-2.6} < \alpha \leq 10^{-1.6}$, and converged correctly above.

Using the upwind scheme with interpolation the method again improves as Δt becomes smaller. The range in which the solution converges increases from, convergence for $\alpha \geq 10^{-1.3}$ with $\Delta t = 1$, to convergence for $\alpha \geq 10^{-3}$ with $\Delta t = 0.01$. Below this region, the solution is either converged or period 2.

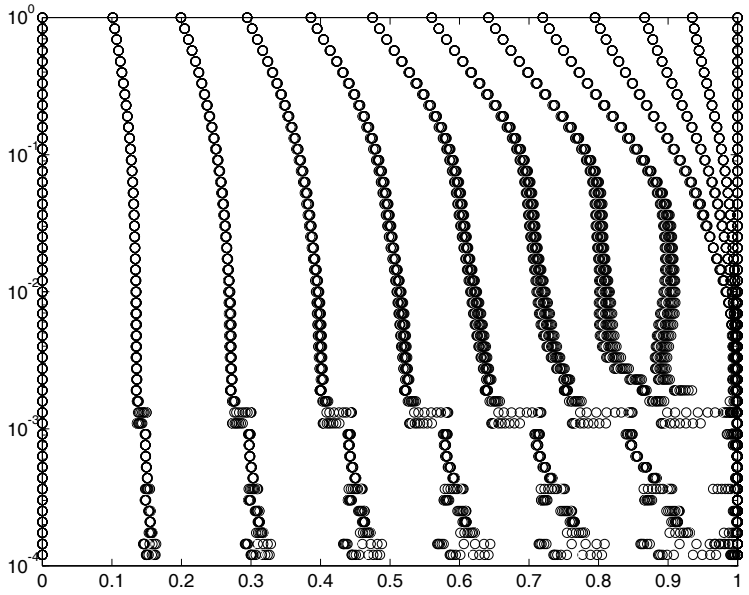

Figure 5.2: Last 10 nodal positions for the linear problem, Tridiagonal iteration, central differences, no interpolation, $\Delta t = 0.001$.

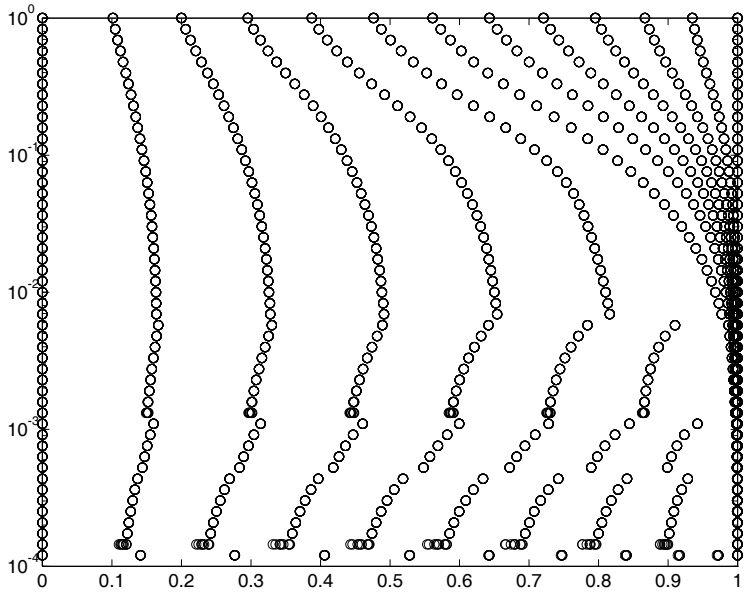

Figure 5.3: Last 10 nodal positions for the linear problem, Tridiagonal iteration, central differences, no interpolation, $\Delta t = 1$.

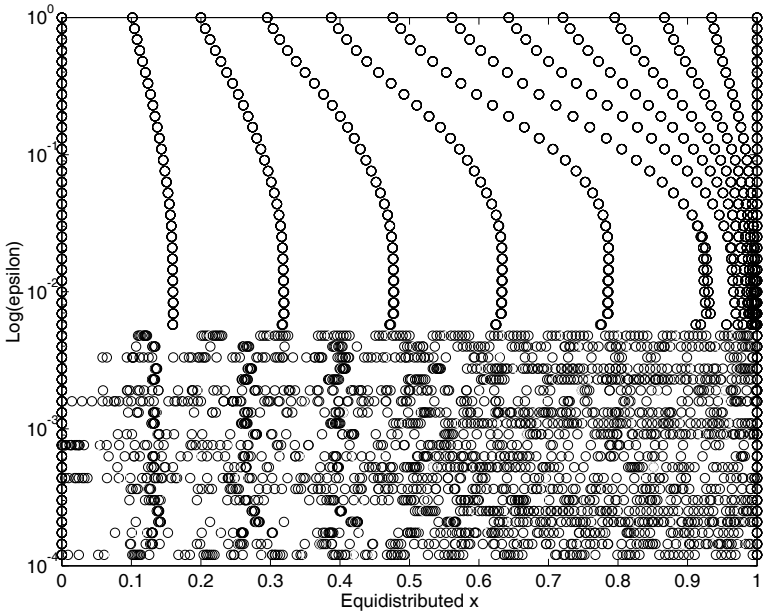

Figure 5.4: Last 10 nodal positions for the linear problem, Ren and Russell iteration, central differences, with interpolation, $\Delta t = 0.01$.

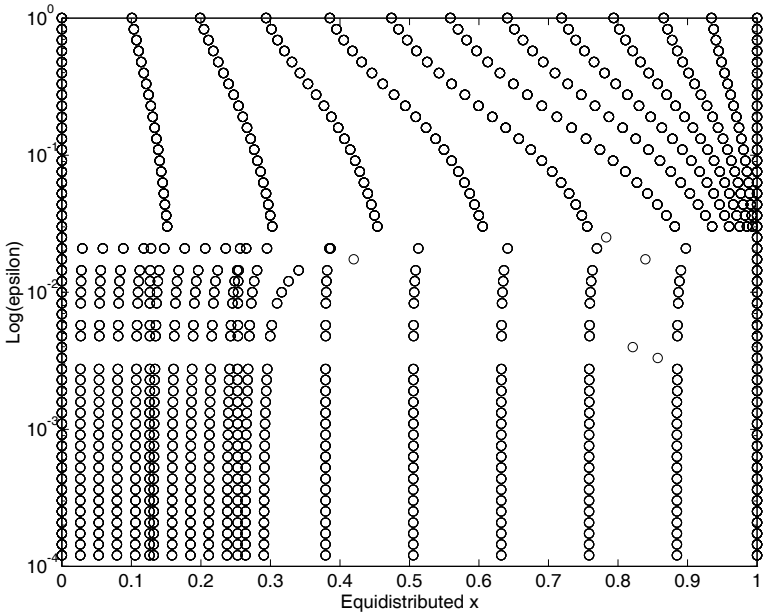

Figure 5.5: Last 10 nodal positions for the linear problem, Ren and Russell iteration, 1st order upwind, no interpolation, $\Delta t = 0.1$.

5.3 Non-Linear Problem

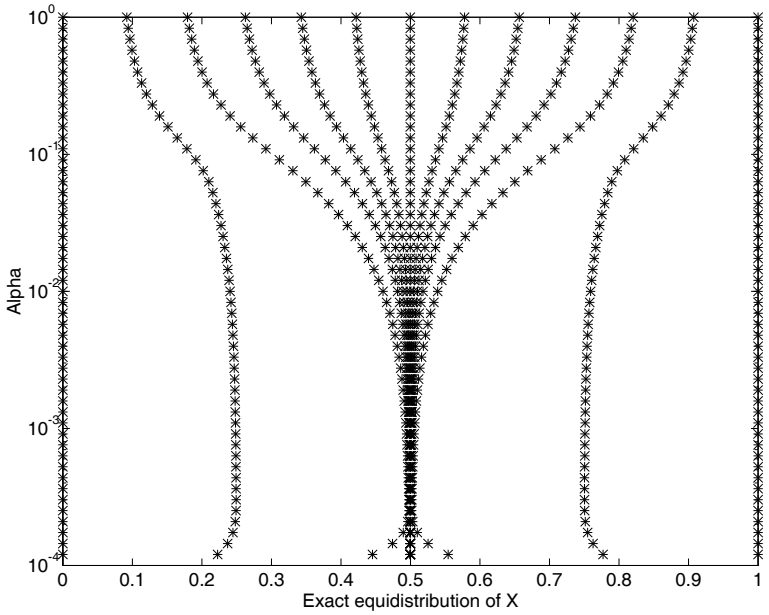

Figure 5.6: "Exact" nodal placements, using fine quadrature, of the steady state solution of the non-linear problem.

5.3.1 Tridiagonal Iteration

Using central differences for the convective term, and no interpolation, this method fails for $\Delta t = 1$ and $\Delta t = 0.1$ when the matrix in the PDE step holding the term $(I - \Delta t J(\boldsymbol{u}^n))$ from Equation (5.9), becomes singular. For $\Delta t = 0.01$ and $\Delta t = 0.001$ there are considerable differences between the results using a skewed initial grid and the results using a symmetric initial grid. Figures 5.7 and 5.8 show the results for $\Delta t = 0.01$. With the skewed initial grid the solution is trying to converge from one side, so the solution is only really converged for $\alpha \geq 10^{-0.9}$, whereas with a symmetric initial grid the solution is correctly converged for $\alpha \geq 10^{-3.2}$. For $\Delta t = 0.001$ the effect of the skewed initial grid is

the same, and with the symmetric grid the tracks have not quite converged for $\alpha \leq 10^{-1.4}$.

When interpolation is performed after each step the method improves considerably and does not fail for any values of α. There are now negligible differences between starting with the skewed or the symmetric initial grid. For the smallest time-step, $\Delta t = 0.001$, the solution has nearly converged into almost parallel tracks. For the other three time-steps, the method improves slightly as Δt decreases; for $\Delta t = 1$ the method only converges for $\alpha \geq 10^{-1.3}$, whereas for $\Delta t = 0.01$ the method is converged for $\alpha \geq 10^{-1.6}$.

Using the 1st order upwind scheme for the convective term, and no interpolation, the method improves as Δt increases. For $\Delta t = 1$ and $\Delta t = 0.1$ the method converges correctly for the full range of ϵ, with either starting grid. For $\Delta t = 0.01$ the method converges completely with the symmetric starting grid, but with the initial grid skewed to the left, the solution moves in from the right (see Figure 5.9). With $\Delta t = 0.001$, the results are similar but for some values of α the solution is slightly unconverged.

When interpolation is used, the results become much worse. For $\Delta t = 0.001$ the solution has nearly converged to almost parallel tracks (as when using central differences and interpolation). For $\Delta t = 0.01$, $\Delta t = 0.1$, and $\Delta t = 1$ the method improves as Δt decreases, but still is never converged for $\epsilon > 10^{-2}$. There are no significant differences between the results with the different starting grids.

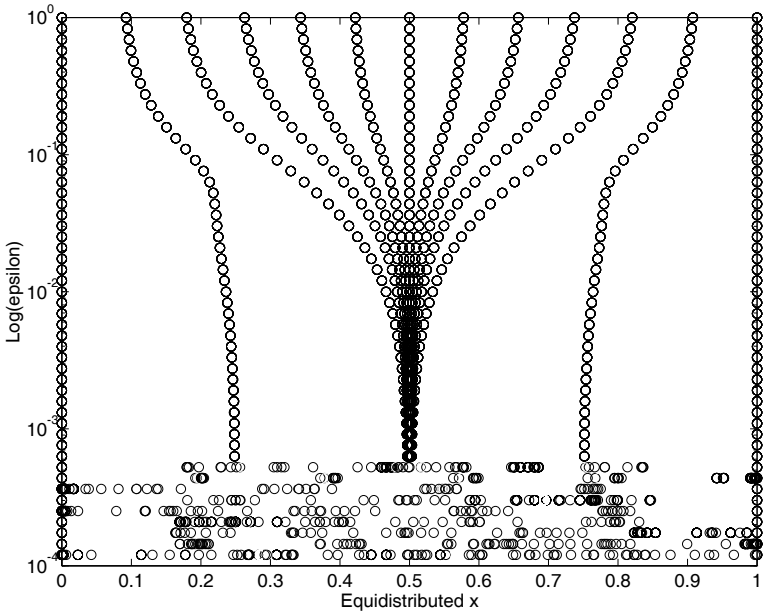

Figure 5.7: Last 10 nodal positions for the non-linear problem, Tridiagonal iteration, central differences, no interpolation, $\Delta t = 0.01$, symmetric starting grid.

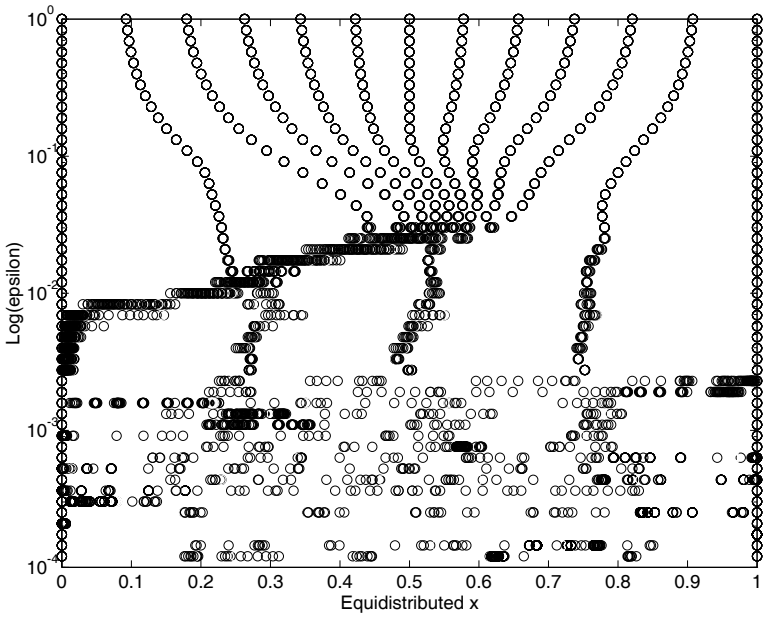

Figure 5.8: Last 10 nodal positions for the non-linear problem, Tridiagonal iteration, central differences, no interpolation, $\Delta t = 0.01$, skewed starting grid.

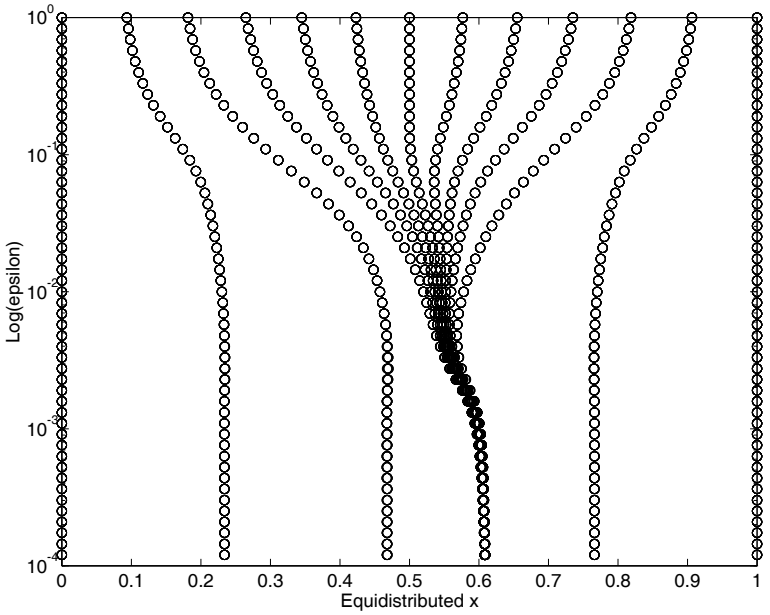

Figure 5.9: Last 10 nodal positions for the non-linear problem, Tridiagonal iteration, 1st order upwind, no interpolation, $\Delta t = 0.01$, skewed starting grid.

5.3.2 Ren and Russell Iteration

With no interpolation, the methods using the two different discretisations of the convective term behave in the same way. For $\Delta t = 1$, $\Delta t = 0.1$, and $\Delta t = 0.01$, the method fails due to the matrix in the PDE step, which holds the term $(I - \Delta t J(\boldsymbol{u}^n))$ from Equation (5.9), becoming singular for many values of ϵ. This occurs with both a symmetric and a skewed starting grid. For $\Delta t = 0.001$ and a skewed starting grid the method fails or is unconverged. With a symmetric starting grid and $\Delta t = 0.001$, the method is unconverged for $\epsilon < 10^{-2.4}$, but converges correctly above.

With interpolation, and using central differences for the convective term, the method fails for $\Delta t = 1$ using both the skewed and the symmetric initial grids.

With $\Delta t = 0.1$ the method is converged for $\alpha \geq 10^{-1.3}$, and with $\Delta t = 0.01$ the method is converged for $\alpha \geq 10^{-1.5}$. When $\Delta t = 0.001$ the method was converged into almost parallel tracks. There was no difference between the results for the two different starting grids.

With interpolation and using 1st order upwind for the convective term, there is again no difference between the results using the two different starting grids. When $\Delta t = 0.001$ the method was converged into almost parallel tracks. Using the other three time-steps, the method improved as Δt decreased.

Chapter 6

Summary

We have investigated three different mesh equidistribution schemes, the tridiagonal iteration, the Ren and Russell iteration, and the nominal iteration. We first looked at the dynamics of these methods when equidistributing a grid to one of four known functions, all of which are dependent on a parameter α. These functions consisted of, a quadratic and a cubic, for which some analysis was possible, and two more complicated functions which were the steady state solutions of the PDEs studied later. In these two cases the parameter α ranged over several orders of magnitude, small values resulting in steep features.

Looking at the equidistribution alone, we found that the tridiagonal and Ren and Russell iterations far out-performed the nominal iteration. It should be noted that computations using the nominal iteration and approximate derivatives were not performed. The improvement in the solutions when the first two iterations were used with the approximate as opposed to the exact derivatives suggest that the performance of the nominal iteration might therefore be improved. However, it was clear when comparing all three methods using exact derivatives that the

nominal iteration was worst.

Spurious dynamics were evident in all three methods. However, this was far less prevalent for the tridiagonal iteration on the simple quadratic and cubic functions. For the other two functions, both the tridiagonal and the Ren and Russell iterations did not appear to exhibit spurious dynamics. However both did give incorrect solutions for small values of the parameter α. In general results did not appear to be heavily dependent on whether there were an odd or an even number of free nodes, nor in general on the initial grid. However, it was noted that in some instances different initial grids could produce different final node placements. This indicates that in some situations the basins of attraction of the solutions have been badly distorted by spurious dynamics.

Next, we used the two more successful iterations, the tridiagonal and the Ren and Russell, coupled with a PDE solver to adaptively solve two time-dependent PDEs to steady state. The first PDE was the linear form of the convection-diffusion equation, which has a boundary layer steady state solution. The second was the viscous Burger's equation, the boundary conditions giving a steep front solution.

Spatial derivatives were discretised using upwind or centred finite differences, whilst an implicit scheme was used for time-stepping in order to avoid over-restrictive stability conditions. Since we were only interested in steady state solutions, no complicated correction of solution values due to grid movement was performed. In particular only linear interpolation or no correction at all were used.

For the linear PDE, the tridiagonal iteration outperformed the Ren and Rus-

sell iteration. The latter converging for a smaller range of the parameter and in a few situations exhibiting spurious dynamics. Qualitatively, the results obtained with or without interpolation were similar. In general, solutions improved with smaller time-steps, however, it was noted that below a certain threshold both accuracy and convergence deteriorated.

For the non-linear PDE, overall, the tridiagonal iteration still performed better than the Ren and Russell itertation. Notably, the Ren and Russell iteration failed in almost all cases where interpolation was not performed, whereas the tridiagonal iteration performed better when interpolation was not used than when it was. For the non-linear problem it was again found that the final node placements could depend on the initial grid used, especially when no interpolation was performed.

Overall, our numerical computations and analysis indicate that, of the three equidistribution schemes studied, the tridiagonal iteration is by far the most robust

Bibliography

[1] D. F. Griffiths, P. K. Sweby and H. C. Yee, "On spurious asymptotic solutions of explicit Runge-Kutta methods." IMA J. Numer. Anal. **12** (1992), 319-338.

[2] J. M. Coyle, J. E. Flaherty and R. Ludwig, "On the Stability of Mesh Equidistribution Strategies for Time-Dependent PDEs." J. Comput. Phys. **62** (1986), 26-39.

[3] Y. Ren and R. D. Russell, "Moving Mesh Techniques Based Upon Equidistribution, and Their Stability." SIAM J. Sci. Stat. Comp. **32** (1992), 1265-1286.

[4] S. Steinberg and P. J. Roach, "Anomalies in Grid Generation on Curves." J Comput Phys. **91** (1990), 255-277.

[5] P. K. Sweby and H. C. Yee, "On the Dynamics of Some Grid Adaption Schemes." RIACS Technical Report **94.02** (1994).

[6] F. Verhulst, "Nonlinear Differential Equations and Dynamical Systems." Springer Verlag 1990.